TECHNICAL MEMORANDUM

49

On the effect of energy/enstrophy conservation in the finite difference scheme of the ECMWF gridpoint model

R. Strüfing

Research Department

January 1982

European Centre for Medium-Range Weather Forecasts
Europäisches Zentrum für mittelfristige Wettervorhersage
Centre européen pour les prévisions météorologiques à moyen

ABSTRACT

A series of forecasts have been carried out with two different finite-difference formulations of the primitive equations of the ECMWF gridpoint model, one scheme conserving potential enstrophy (standard version) and the other energy. The similarity of the results after 10 days suggests that for a high resolution model with sophisticated subgrid parameterization, conservation of enstrophy is not essential for medium range forecasts.

1. INTRODUCTION

Sadourny (1975) compared the results of integrations with two shallow water models. One model conserved potential enstrophy, the other, energy. He found that at a critical dissipativity the enstrophy conserving model was significantly more stable than the energy conserving model. Since the critical dissipativity was much smaller for the formulation conserving potential enstrophy this model can be used for very long integrations with negligible loss of energy in the scales of meteorological interest.

Based on these results the finite-difference scheme for the ECMWF gridpoint model was designed to conserve enstrophy. However, in order to investigate the impact of conservation principles on forecasts with the ECMWF gridpoint model the finite-difference formulation of the primitive equations has been modified such that it conserves energy instead of potential enstrophy. This energy conserving scheme differs from Sadourny's in that it uses the advective form of the equations and conserves momentum under advection processes.

Furthermore it is of interest to compare the results given by the energy conserving version of the ECMWF model with those of the GFDL model, since the latter also conserves energy, although it uses an unstaggered Arakawa A grid.

This report compares four integrations over 10 days and one over 30 days carried out with both versions of the ECMWF model. The results of two GFDL integrations are also discussed.

2. MATHEMATICAL FORMULATION OF THE ENERGY CONSERVING FINITE-DIFFERENCE SCHEME

Since the existing finite-diffference scheme of the ECMWF gridpoint model is already energy conserving in the vertical coordinate only the "horizontal" parts of momentum equations have to be modified. In the following therefore these equations are written in their barotropic form only. The scheme is basically that of Lilly (1965).

In the continuous form the equations are written as follows.

Momentum

$$\frac{\partial u}{\partial t} + \frac{u}{a\cos\theta}\,\frac{\partial u}{\partial \lambda} + \frac{u}{a}\,\frac{\partial u}{\partial \theta} - \left(f + \frac{u}{a}\tan\theta\right) v + \frac{1}{a\cos\theta}\,\frac{\partial \phi}{\partial \lambda} = 0 \tag{1}$$

$$\frac{\partial v}{\partial t} + \frac{u}{a\cos\theta}\,\frac{\partial v}{\partial \lambda} + \frac{u}{a}\,\frac{\partial v}{\partial \theta} + \left(f + \frac{u}{a}\tan\theta\right) u + \frac{1}{a}\,\frac{\partial \phi}{\partial \theta} = 0 \tag{2}$$

Continuity equation

$$\frac{\partial \phi}{\partial t} + \frac{1}{a\cos\theta}\left(\frac{\partial}{\partial \lambda}(\phi u) + \frac{\partial}{\partial \theta}(\phi v\cos\theta)\right) = 0 \tag{3}$$

the finite-difference momentum equations on the staggered Arakwa-C-grid are:

$$\frac{\partial u}{\partial t} = - \frac{1}{a\cos\theta\bar{\phi}^{\lambda}} \left(\overline{\bar{U}^{\lambda}\delta_{\lambda}u}^{\lambda} + \overline{\overline{V\cos\theta\delta_{\theta}u}^{\lambda}}^{\theta} \right) + \text{Coriolis}_u - \frac{1}{a\cos\theta}\delta_{\lambda}\phi \tag{4}$$

$$\frac{\partial v}{\partial t} = - \frac{1}{a\cos\theta\bar{\phi}^{\theta}} \left(\overline{\bar{U}^{\theta}\delta_{\lambda}v}^{\lambda} + \overline{\overline{V\cos\theta}^{\theta}\delta_{\theta}v}^{\theta} \right) - \text{Coriolis}_v - \frac{1}{a}\delta_{\theta}\phi \tag{5}$$

where: $U = \bar{\phi}^{\lambda} u$

$$\cos_{\theta} V = \overline{\phi\cos\theta v}^{\theta}$$

$$\text{Coriolis}_u \qquad \frac{1}{\bar{\phi}^{\lambda}\cos} \overline{\left(f \cos\theta + \frac{\bar{u}^{\theta}}{a}\sin\theta \right) \bar{V}^{\lambda}}^{\theta}$$

$$\text{Coriolis}_v \qquad \frac{1}{\overline{\phi\cos\theta}^{\theta}} \overline{\left(f \cos\theta + \frac{\bar{u}^{\theta}}{a}\sin\theta \right) \bar{U}^{\theta}}^{\lambda}$$

Energy conservation under advection processes is easily proved and the symmetric formulation of the Coriolis terms guarantees formally conservation of energy by one complete scheme.

There are no problems to apply this scheme at the poles.

3. SUBJECTIVE AND OBJECTIVE ASSESSMENT

The four 10 day forecasts carried out with the two models are from the 16.1.1979, 1.3.1965, 22.2.1981 and the 1.1.1977, the latter integration being extended to 30 days. Two forecasts with the GFDL model are available for the 1.3.1965 and 1.1.1977

3.1 Synoptic evaluation and scores

3.1.1 10 day forecasts

A series of 500 mb and 1000 mb geopotential height field charts for day 10 are presented as well as the time evolution of the anomaly correlation of the geopotential height.

16.1.1979

After 10 days the geopotential height fields (Fig. 1) show very small insignificant differences only. This similarity of the integrations with the two different conserving schemes is confirmed by the anomaly correlations (Fig. 2) which show a marginally higher correlation for the enstrophy conserving scheme.

1.3.1965

Though the predictability for this forecast is not as high as that for the 16.1.1979, the differences in the geopotential height (Fig. 3) are again very small. There are no phase differences, but the low over nothern Europe is simulated better by the energy conserving scheme. However, the anomaly correlation (Fig. 4) indicates a slight advantage for the enstrophy conserving model. The low northeast of the Caspian Sea in the energy conserving forecast resembles more the one produced by the GFDL integration (see ECMWF Technical Report No.1). These two forecasts developed a cut-off low, whereas the enstrophy conserving ECMWF model maintains a trough.

22.2.1981

This initial data had the new ECMWF orography and we confirm the results, that the formal conservation properties of energy or enstrophy do not influence significantly the 10 day forecast. The only interesting difference in the charts of geopotential height (Fig. 5) are the lows over the East-Pacific which are split into two centres in the energy conserving forecast. The anomaly correlation (Fig. 6) shows again a small advantage for the enstrophy conserving scheme, but for Day 6-8 only.

1.1.1977

The patterns in the geopotential height fields (Fig. 7) are again very similar, but the different tilts in the troughs and ridges over the Atlantic leave the possibility of a rapid growth of the deviations between the two models.

3.1.2 30 day integration

The 10-day forecast from the 1.1.1977 were extended to 30 days. Fig. 9 presents the geopotential height fields at day 15. At this range the two forecasts differ considerably. It seems that the enstrophy conserving model only carries some skill over the area of the Pacific and North America.

A comparison of the mean geopotential height charts for the last 10 days (Fig. 10a-b) indicates that the enstrophy conserving forecast performs better in the longer range, although both models are similar in their major deficiencies. In this period the gradients in the 1000 mb height charts in the energy conserving integration are slightly weaker. It is interesting, that the enstrophy conserving model establishes a synoptic situation over northern Europe and west Russia which is close to a blocking, agreeing with the analyses rather better than the energy conserving model.

The 30-day mean geopotential height fields in Fig. 11a-b are again similar. The phase differencesin the long waves of the two integrations are insignificant, whereas the energy conserving scheme develops higher amplitudes, due to which it shows worse results in the difference maps. Both ECMWF integrations verify significantly worse than the GFDL model (Fig. 12).

3.2 Evaluation of kinetic energy and zonal means of temperature and zonal wind

According to Sadourny (1975) for shallow water models with simple dissipative mechanisms the different constraints for the finite difference schemes have a a major role in the transfer of kinetic energy into the smaller scales. However, in case of 10 day forecasts with the baroclinic ECMWF gridpoint model the spectra of kinetic energy (Fig. 13a-d) do not show systematic differences in the wavenumbers 10-20. Calculations for the wavenumbers 20-80 which are not presented here, indicated no systematic differences in the spectra of kinetic energy. It seems that the enstrophy conserving scheme has slightly more kinetic energy in the first 10 wavenumbers.

The time evolution of the total kinetic energy (Fig.14a-d) is not influenced by the different constraints, but in the latter stages of the forecasts the kinetic energy in the wavenumber 4 to 9, the baroclinic waves, is higher in the enstrophy conserving scheme. The differences at day 0 in Fig. 14a and d are due to some changes in the calculation of virtual temperature.

All the other objective scores and diagnostics available did not indicate any significant differences for the 10-day forecasts.

The spectra for the kinetic energy for the last 15 days of the 30 day integrations confirm the results derived from the 10-day forecasts. Fig. 16 presents the zonal means for the deviations of temperature and the zonal component of the wind from verifying analysis. There is slightly stronger cooling for the energy conserving integration in the troposphere and the northern stratosphere. The wind deviations north of 60°N are higher for this model, but lower at the tropopause at 20°N.

Sensible heat flux (Fig. 17) and momentum flux (Fig. 18) are smaller for the energy conserving scheme and slightly more realistic.

A subjective assessment of the rainfall maps of both forecasts showed that the change of conservation properties does not influence the rainfall.

4. CONCLUSIONS

This series of forecasts indicate that for a high resolution gridpoint model with sophisticated subgrid scale parameterization the impact of the formal conservation of potential enstrophy or energy, respectively, does not become apparent for a 10 day forecast and is of minor influence. For the 30 day integrations it was shown that significant deviations between the two integrations occurred around day 15, though the 30-day-means of geopotential height were similar.

In agreement with Sadourny (1975) the enstrophy conserving scheme is better. At day 10 the anomaly correlations of this model were slightly higher and at day 15 it has more skill at 500 mb. In the latter stages of the 30 day integration the enstrophy conserving scheme had higher scores, though the error patterns were similar. Results, not shown in this report lead to the conclusion that the differences in the results of the two models increase with decreasing resolution.

Because of the small differences in the two series of integrations it could not be shown whether the results of one of the two ECMWF models are more similar to the GFDL integrations.

No significant differences in the spectra of kinetic energy were found. A possible reason is that the energy transfer into smaller scales is far more controlled by the dissipative mechanisms of the model than by the constraints in the finite difference scheme. Mean charts for the geopotential height showed for the 30 day integration a weaker gradient for the energy conserving model.

References

K.Arpe, L.Bengtsson, A.Hollingsworth, Z.Janjic 1976 A case of a 10 day prediction, ECMWF Technical Report No.1.

D.M. Burridge 1979 Some aspects of large scale numerical modelling of the atmosphere. ECMWF Seminar Proceedings, 1979, Vol.2.

ECMWF Forecast Model Documentation Manual

D.K. Lilly 1965 On the computational stability of numerical solutions of time-dependent non-linear geophysical fluid dynamics problems. Mon.Wea.Rev., -93, 11-25.

K.Miyakoda, personal communication, (to be published.)

R.Sadourny 1975 The dynamics of finite-difference models of the shallow-water-equations. J.Atm.Sci., -32, 680-689.

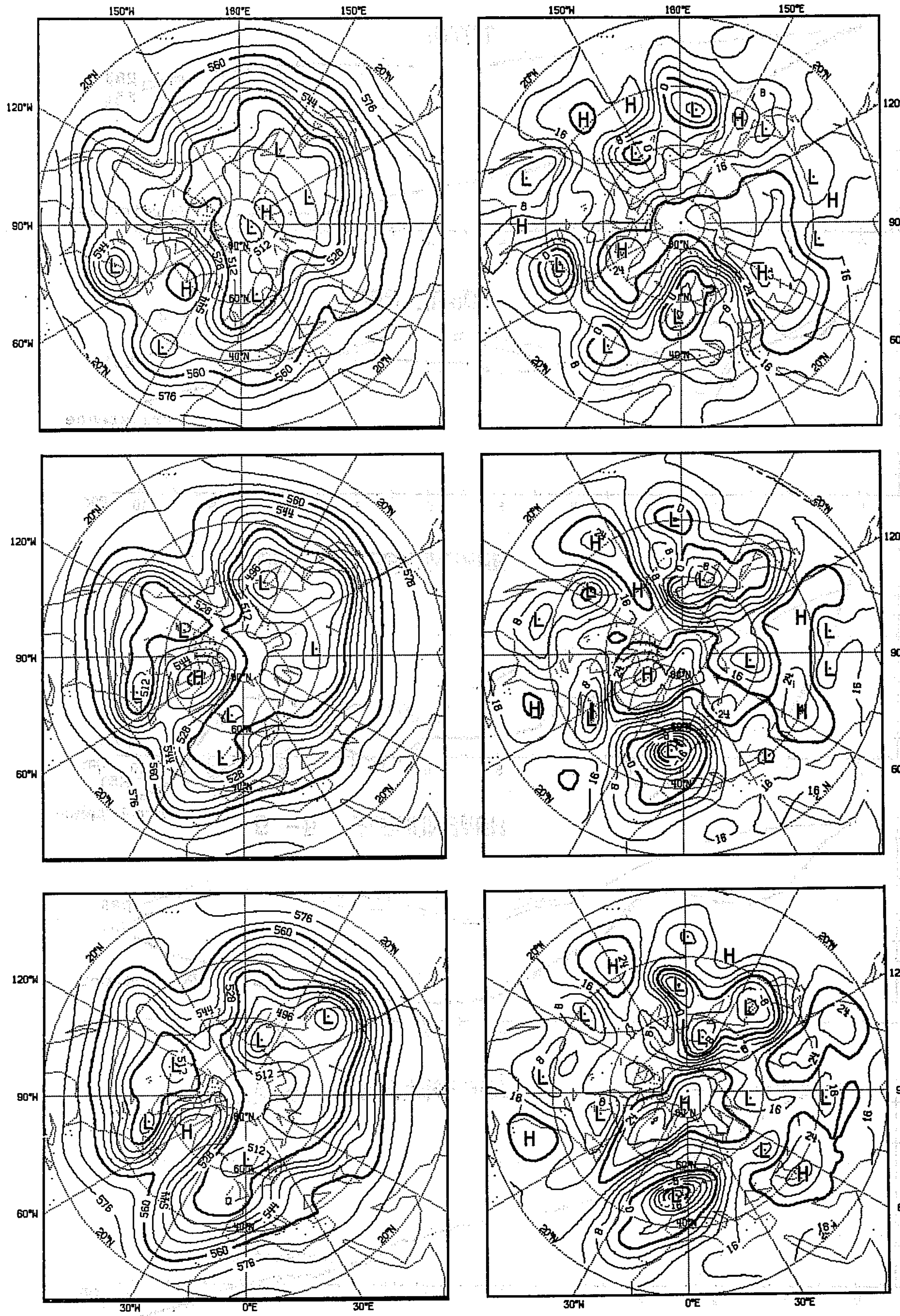

Fig. 1 Northern Hemisphere geopotential fields for 500 mb (left) and 1000 mb (right) at day 10 of 16.1.79 for verifying analysis (top), energy (centre) and enstrophy conserving forecasts (bottom).

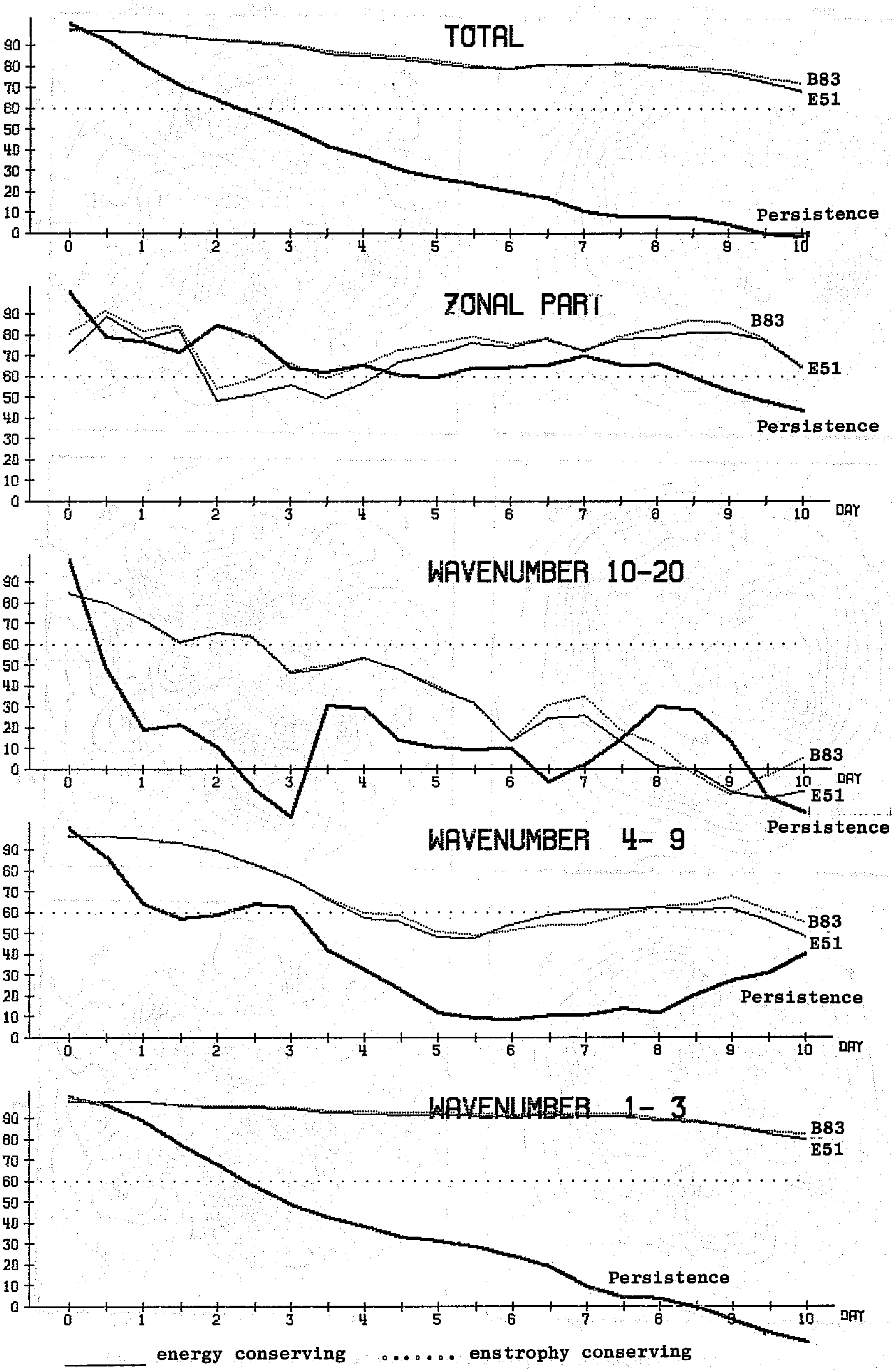

Fig. 2 Anomaly correlation coefficients of the height field for the 16.1.79 for energy and enstrophy conserving forecasts mean for the troposphere 1000-200 mb and 20 - 82.5^{o}N.

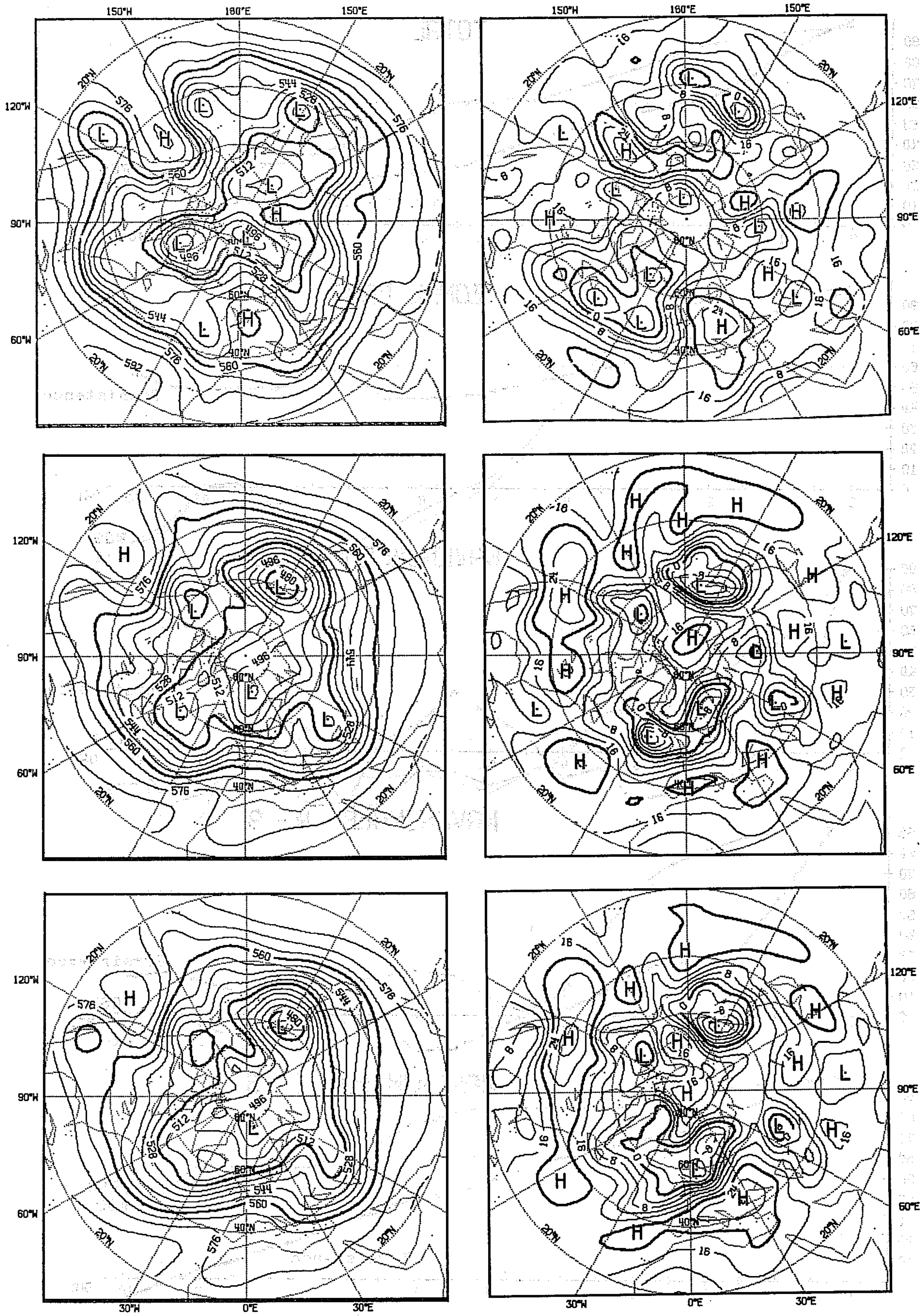

Fig. 3 Northern Hemisphere geopotential fields for 500 mb (left) and 1000 mb (right) at day 10 of 1.3.65 for verifying analysis (top), energy (centre) and enstrophy conserving forecasts (bottom).

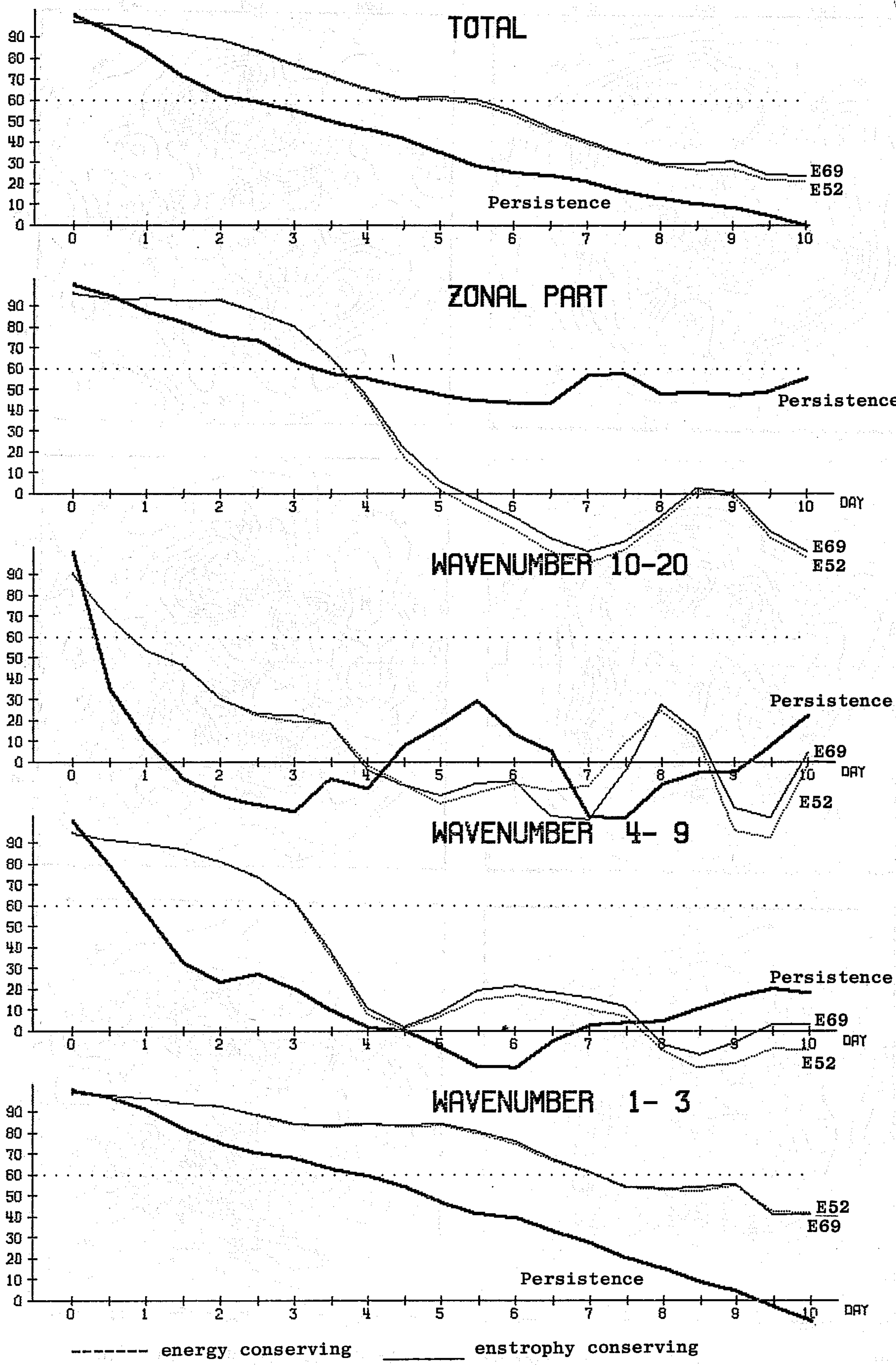

Fig. 4 Anomaly correlation coefficients of the height field for the 1.3.79 for energy and enstrophy conserving forecasts mean for the troposphere 1000-200 mb and 20 - 82.5^{o}N.

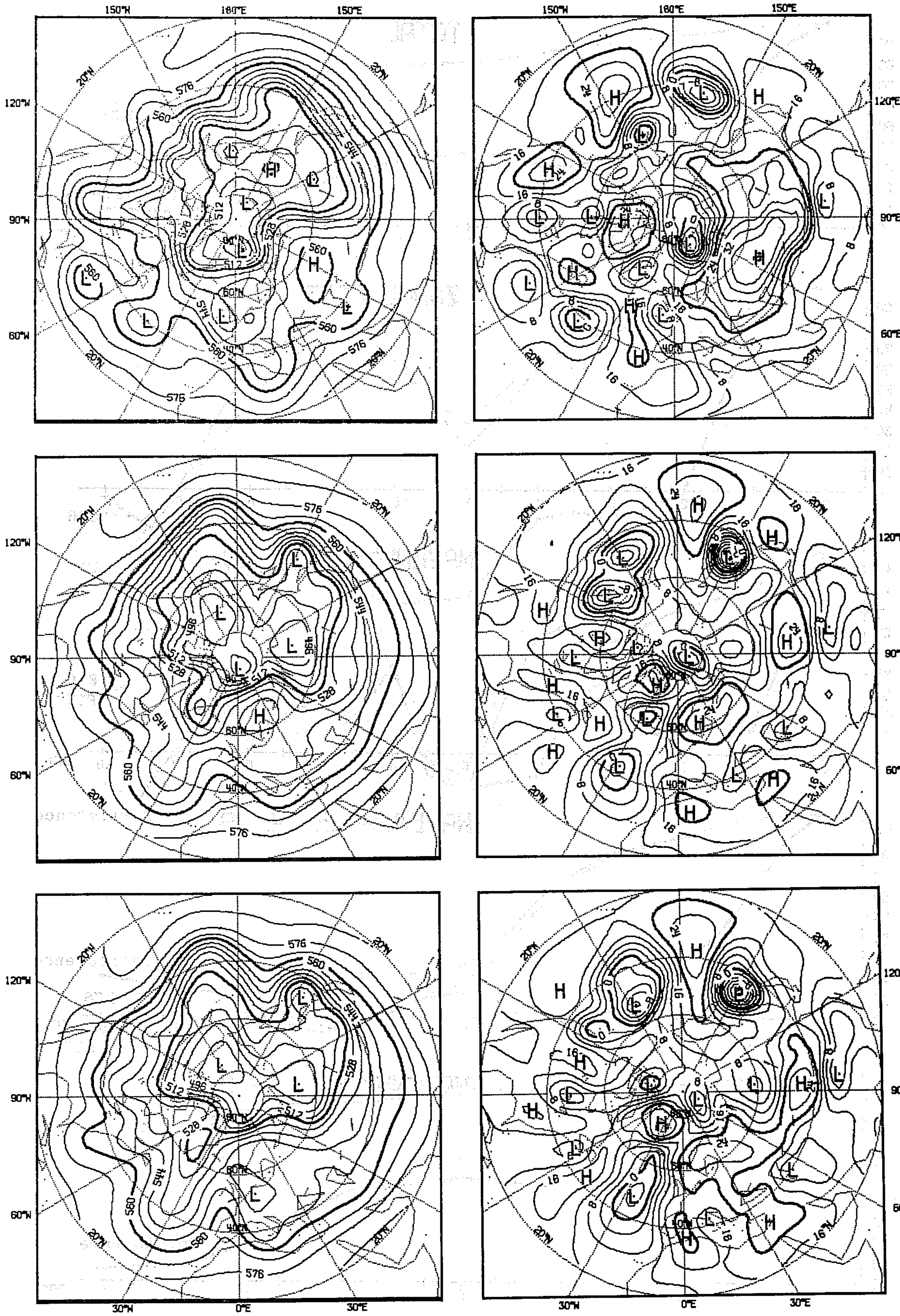

Fig. 5 Northern Hemisphere geopotential fields for 500 mb (left) and 1000 mb (right) at day 10 of 12.2.81 for verifying analysis (top), energy (centre) and enstrophy conserving forecasts (bottom).

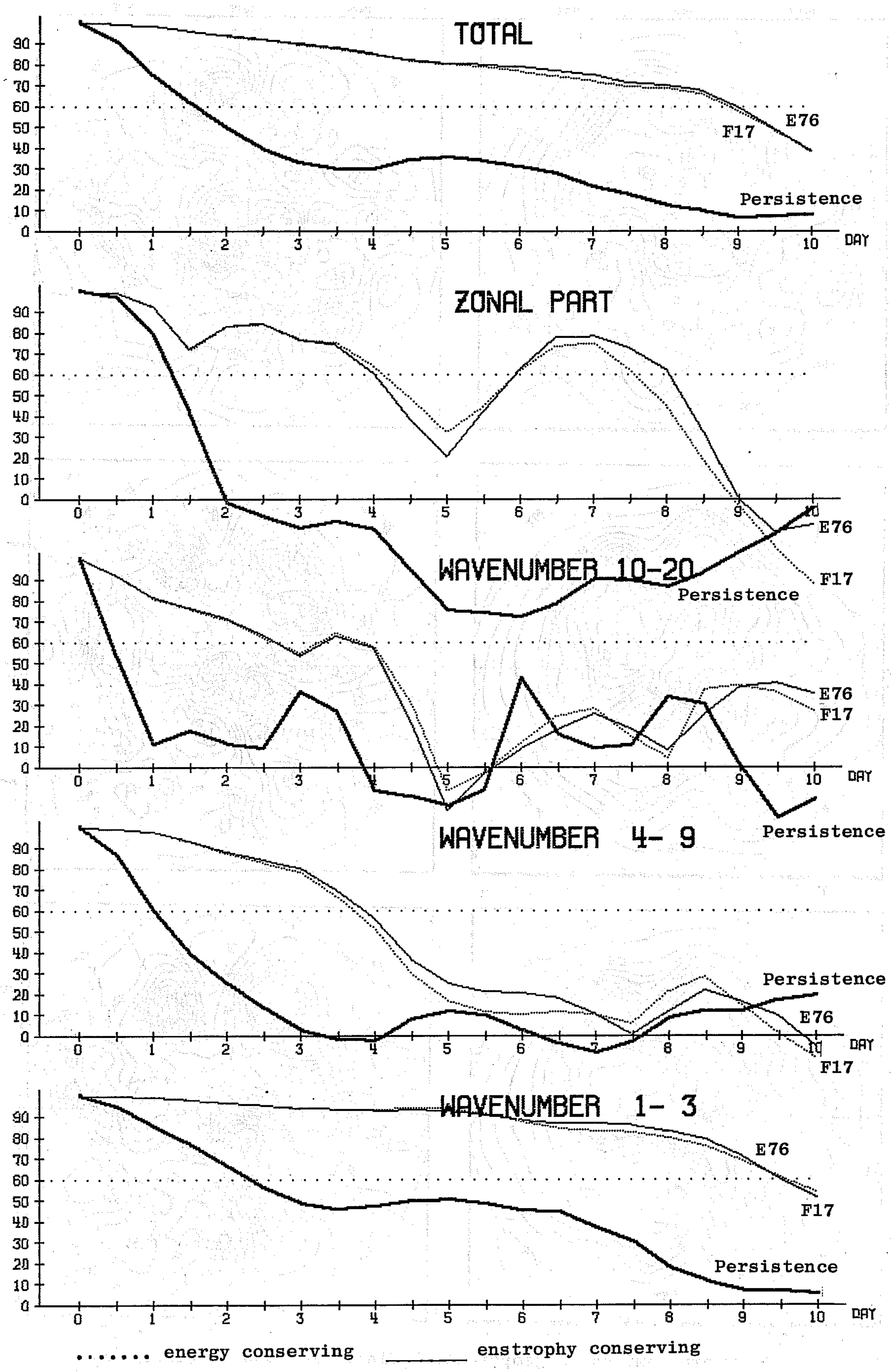

Fig. 6 Anomaly correlation coefficients of the height field for the 12.2.81 for energy and enstrophy conserving forecasts mean for the troposphere 1000-200 mb and 20 - 82.5°N

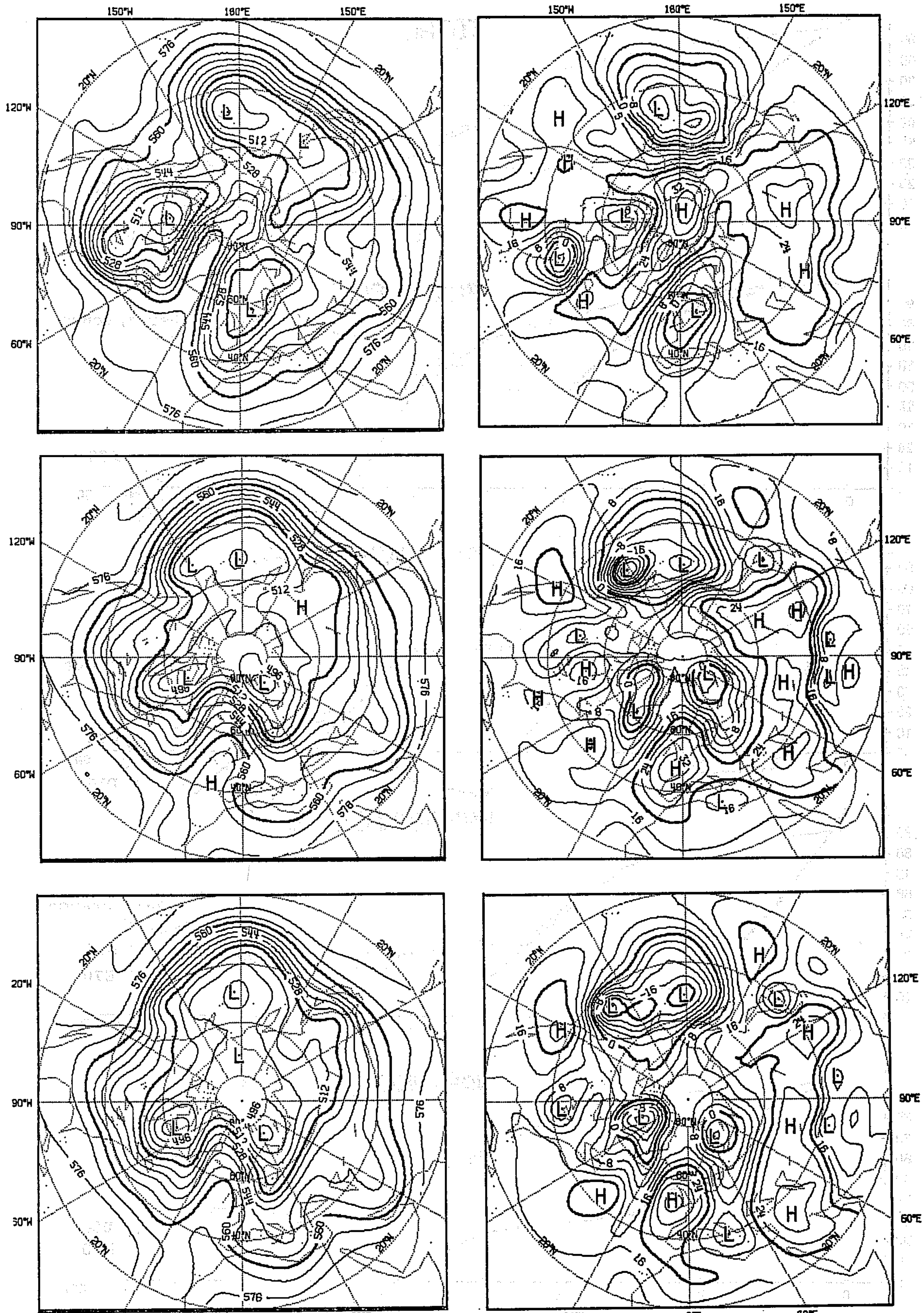

Fig. 7 Northern Hemisphere geopotential fields for 500 mb (left) and 1000 mb (right) at day 10 of 1.1.77 for verifying analysis (top), energy (centre) and enstrophy conserving forecasts (bottom).

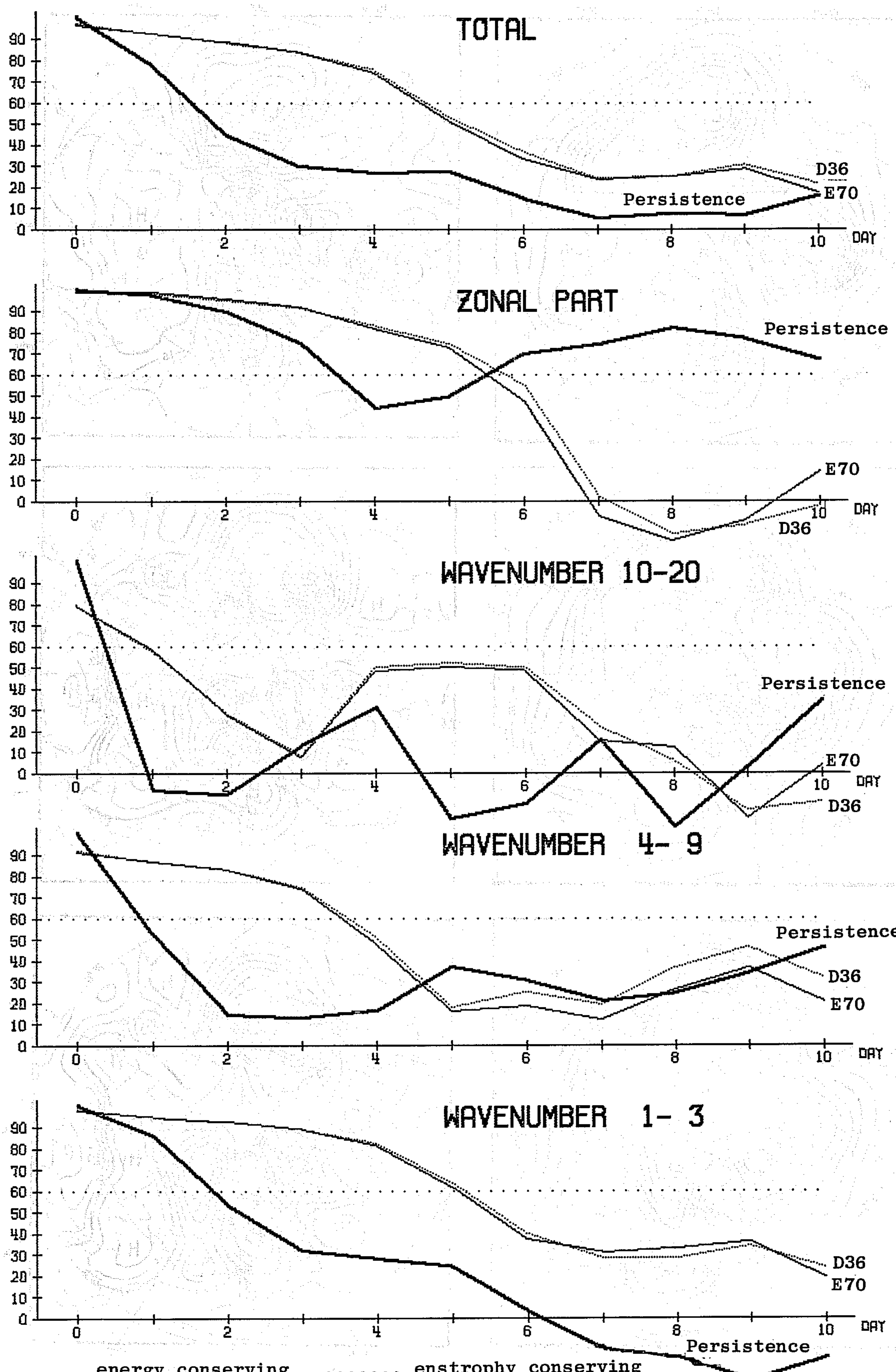

Fig. 8 Anomaly correlation coefficients of the height field for the 1.1.77 for energy and enstrophy conserving forecasts mean for the troposphere 1000-200 mb and 20 - 82.5°N.

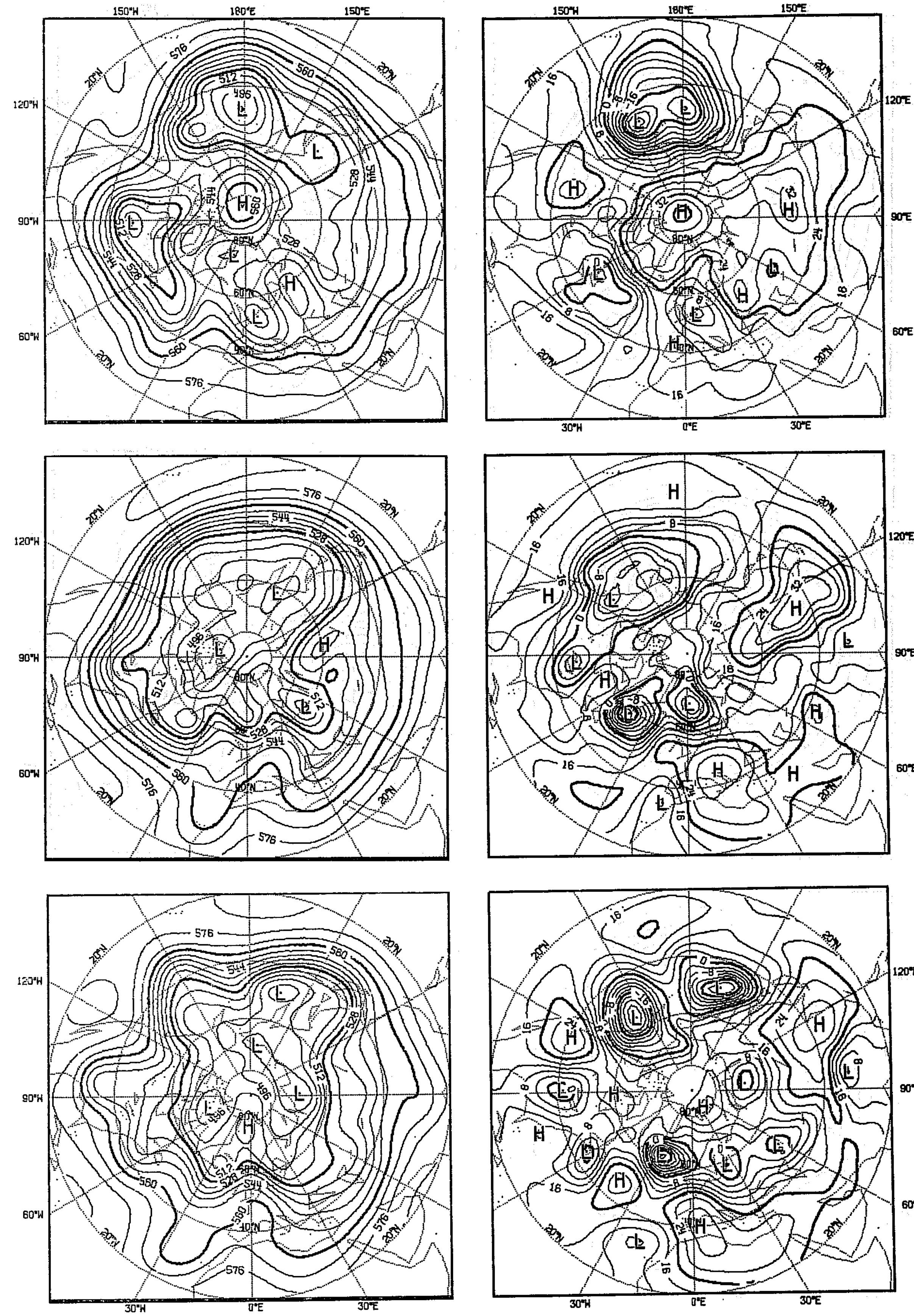

Fig. 9 Northern Hemisphere geopotential fields for 500 mb (left) and 1000 mb (right) at day 15 of 1.1.77 for verifying analysis (top), energy (centre) and enstrophy conserving forecasts (bottom).

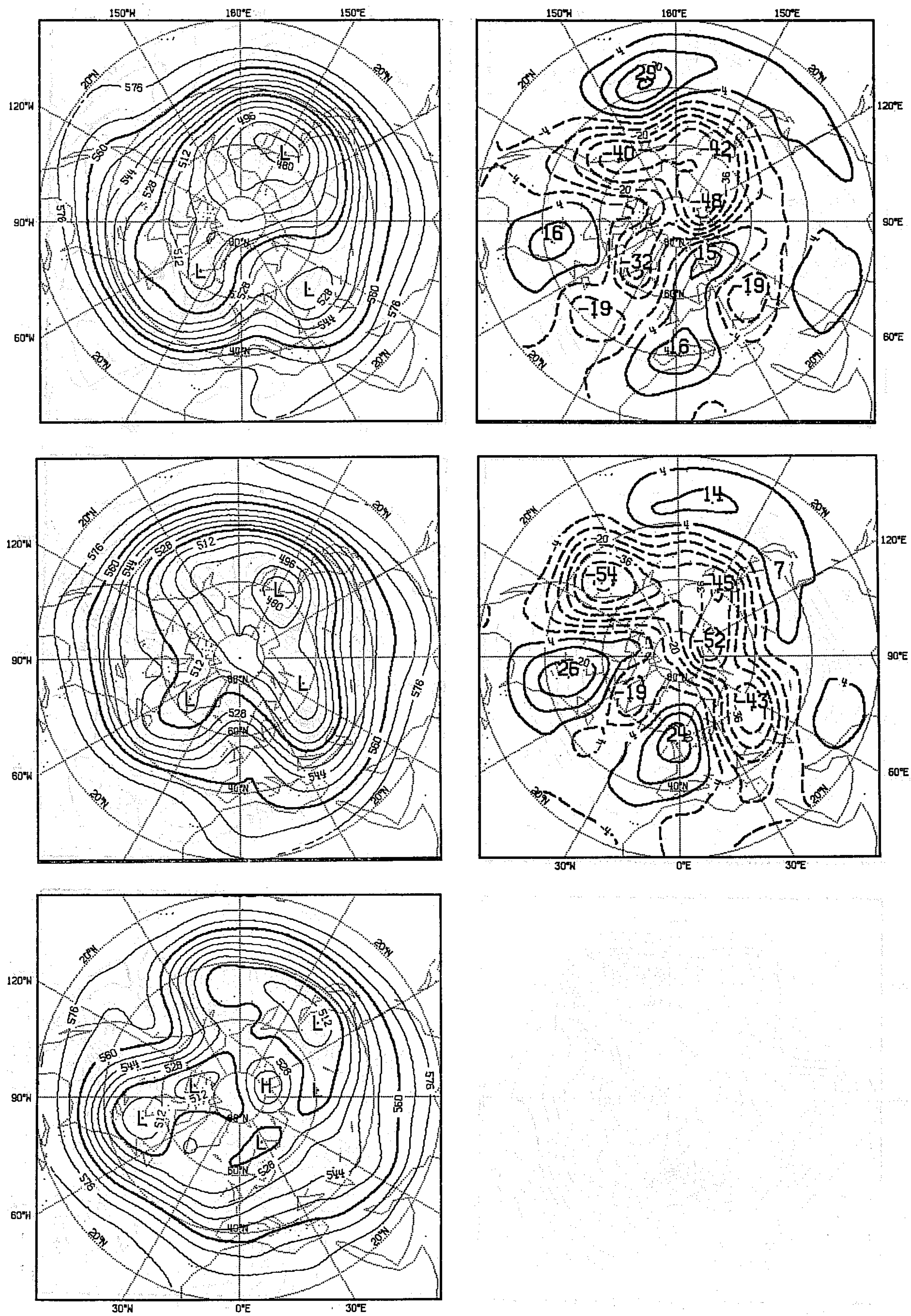

Fig. 10a Northern Hemisphere geopotential fields (left) for 500 mb for day 21 to 30 of the 1.1.77 for enstrophy (top), energy conserving (centre) forecasts and verifying analysis (bottom) and differences forecasts - analysis (left).

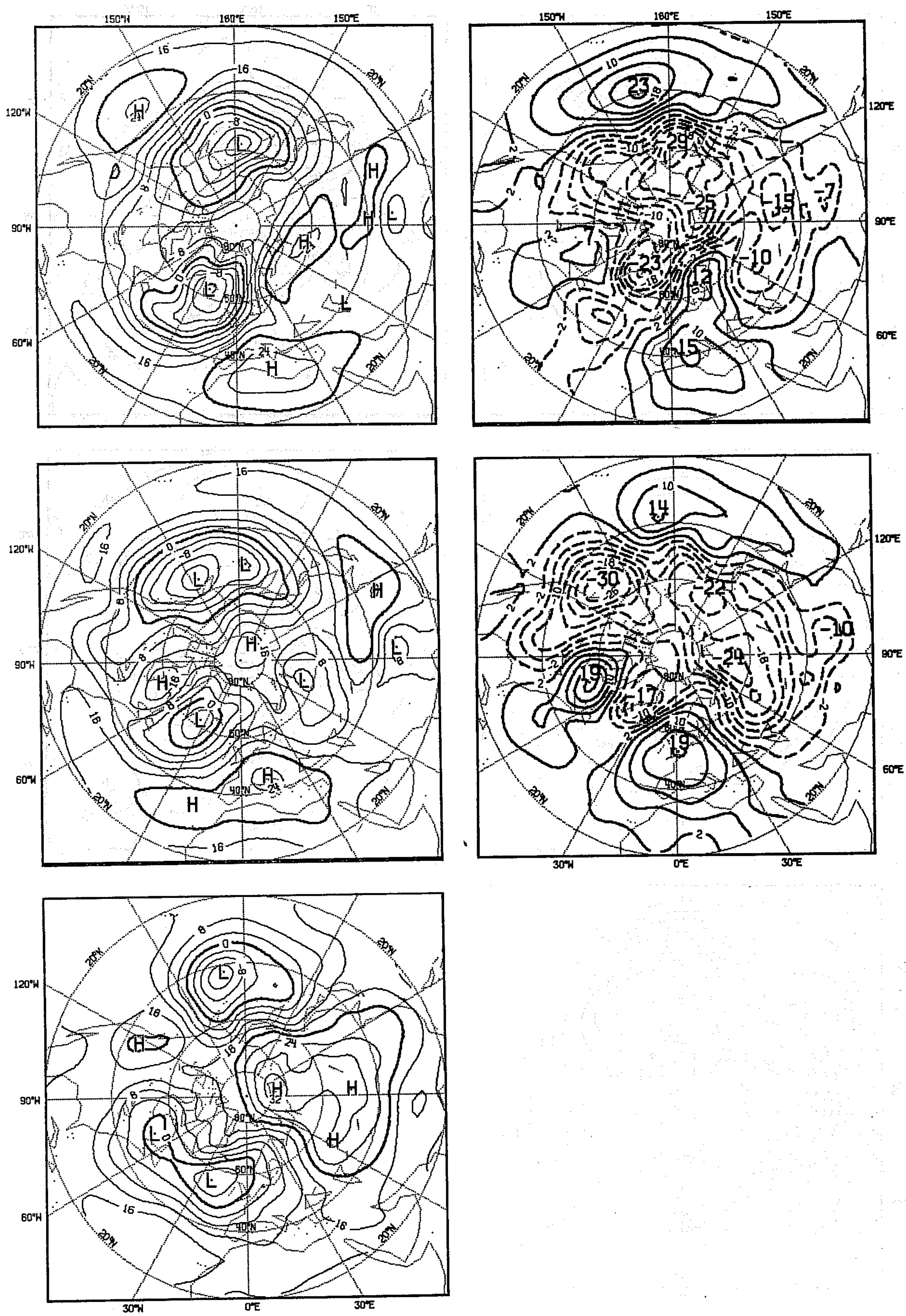

Fig. 10b As for Fig. 10a but for 1000 mb.

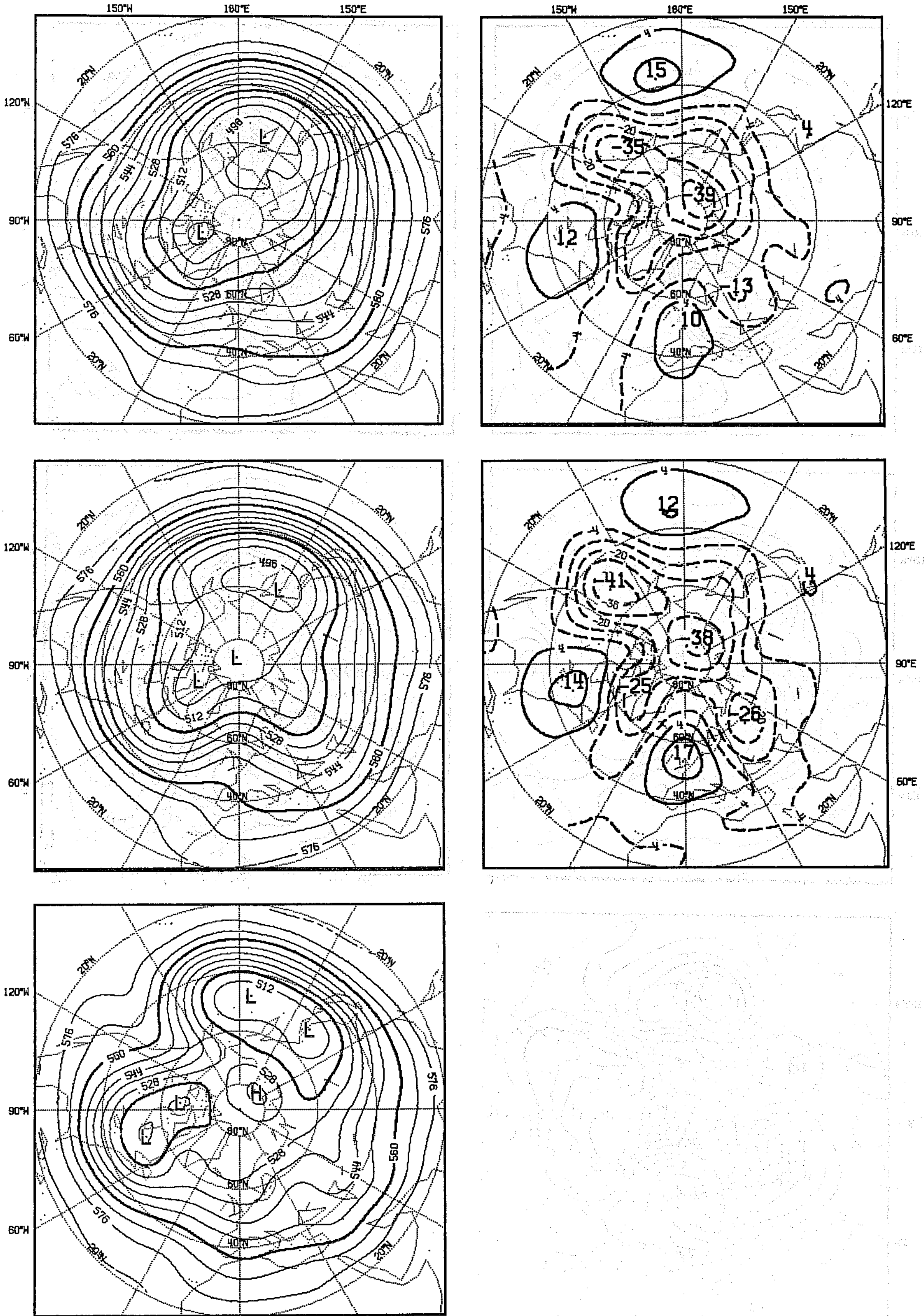

Fig. 11a As for Fig. 10a for 30 day mean.

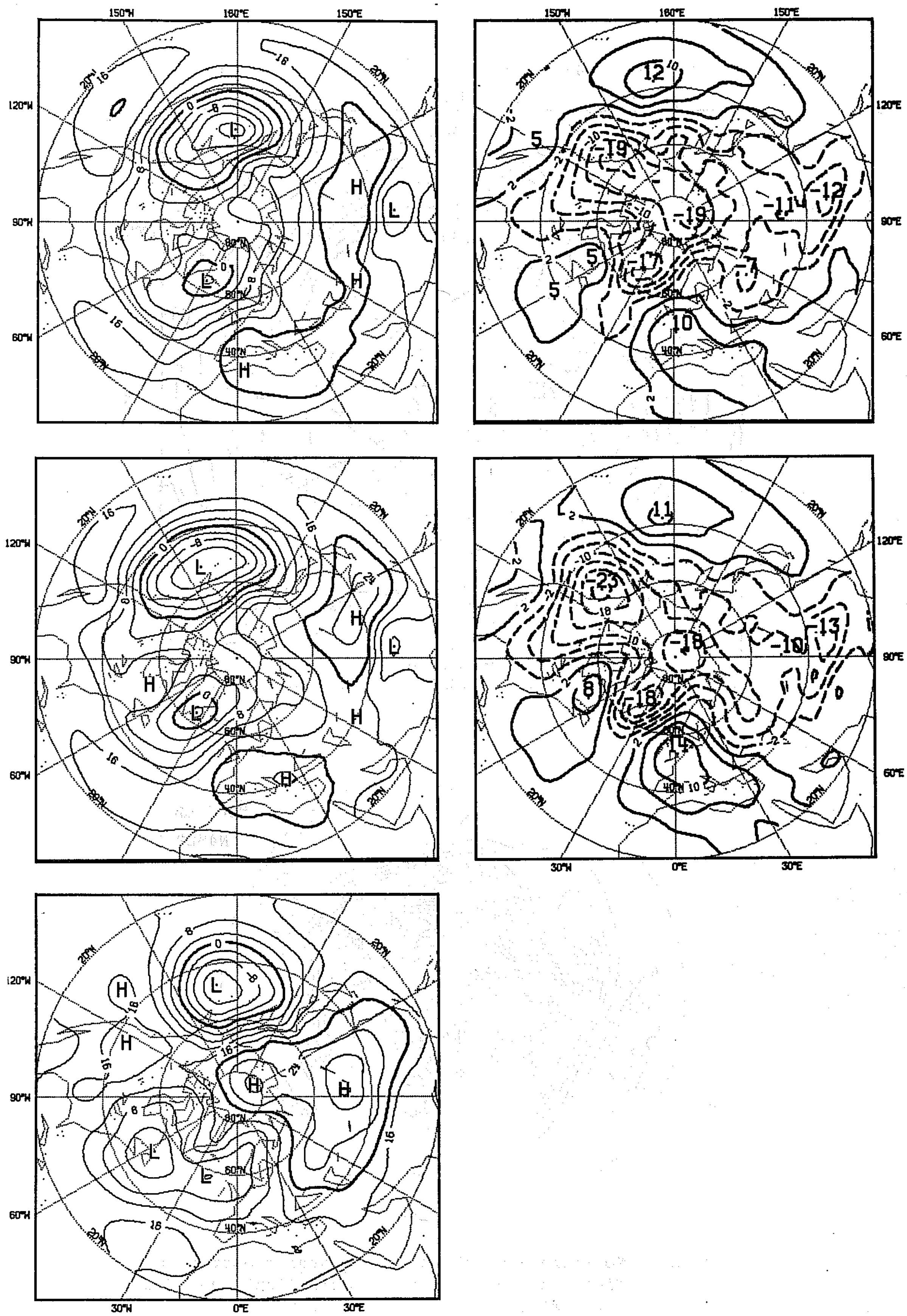

Fig. 11b As for Fig. 10b but 30 day mean.

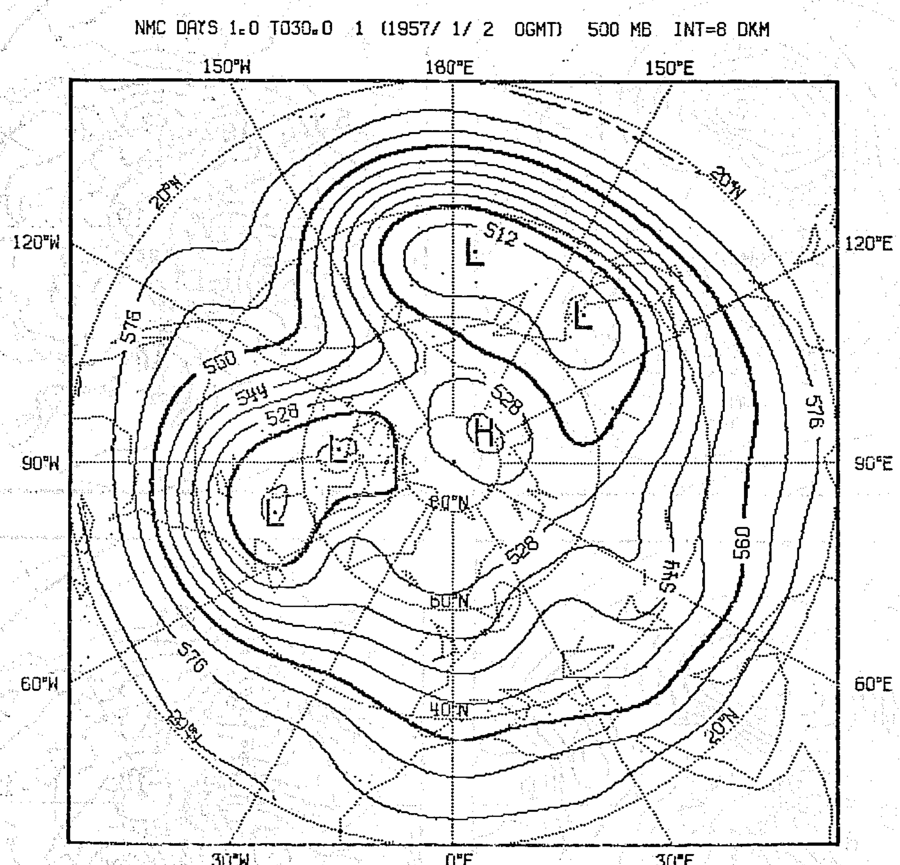

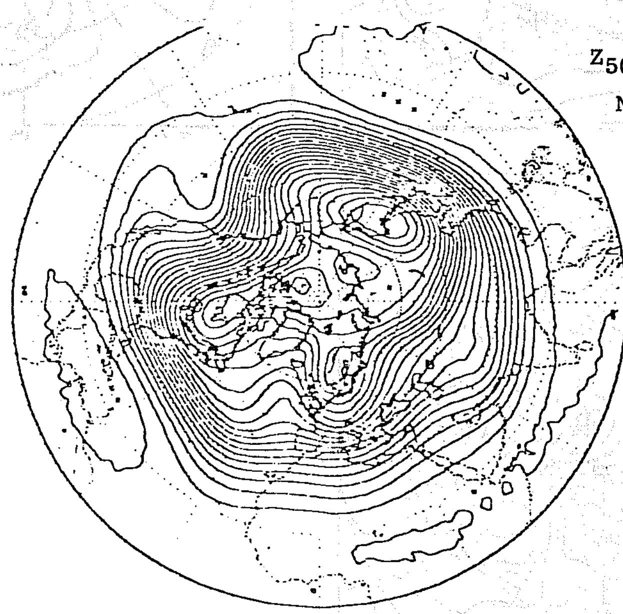

Fig. 12 Northern Hemisphere 30 day mean geopotential fields for verifying analysis (top) and GFDL forecast (bottom) of the 1.1.77.

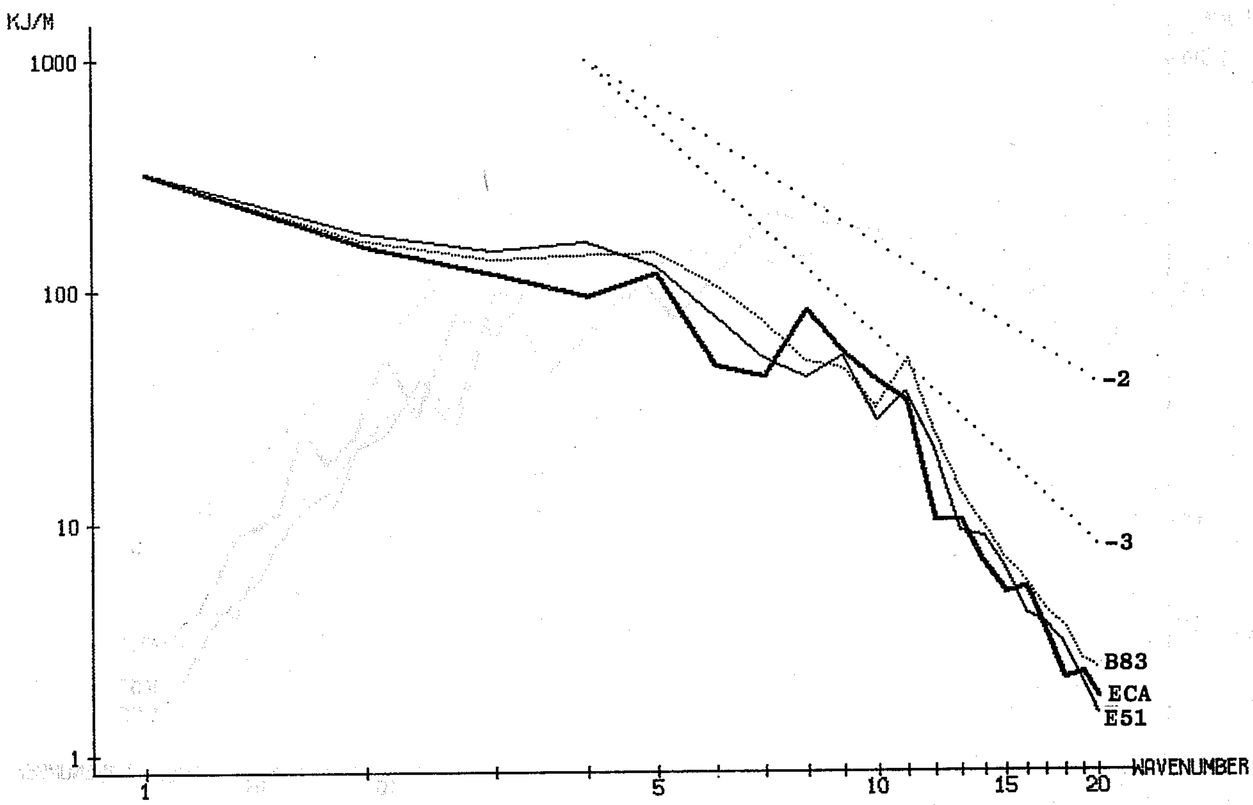

_______ energy conserving .... enstrophy conserving

Fig. 13a Spectra of kinetic energy for the 16.1.79 mean between 40 and 60°N and over 1000 to 200 mb.

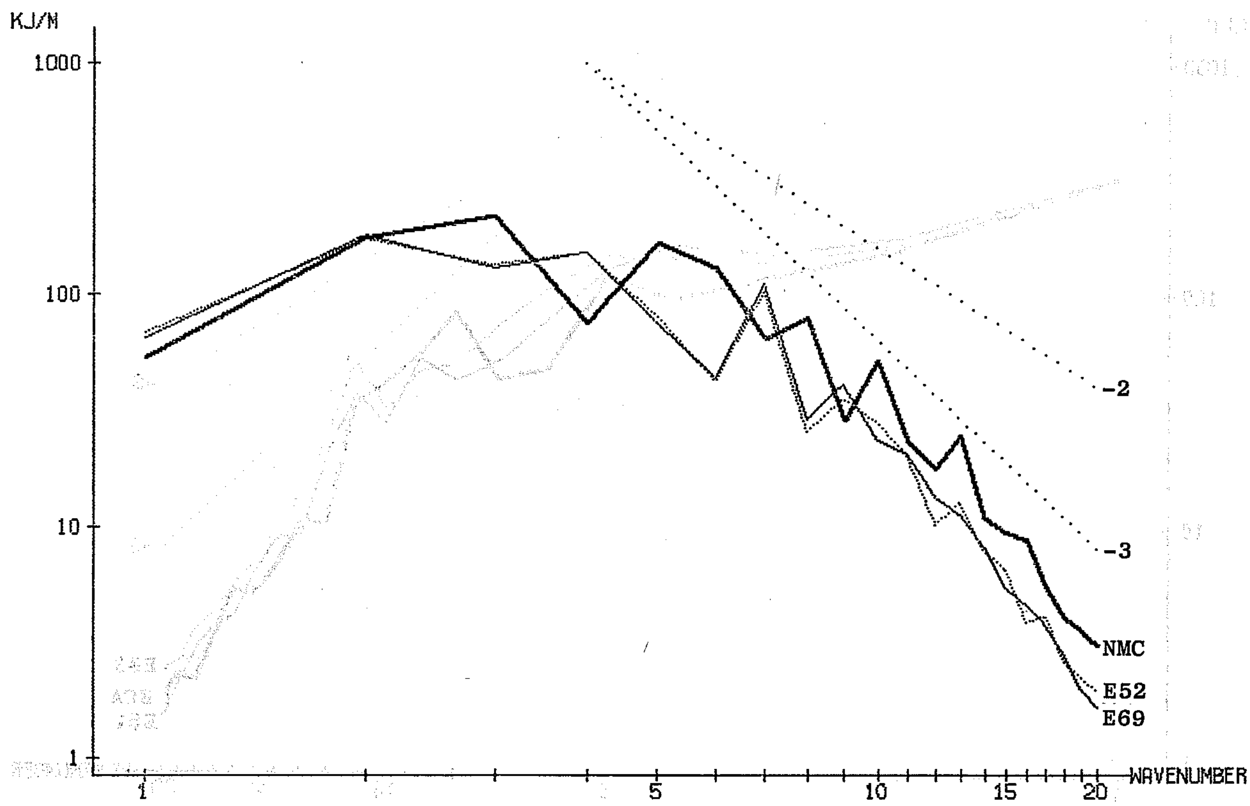

.... energy conserving ________ enstrophy conserving

Fig. 13b As for Fig. 13a but for 1.3.65.

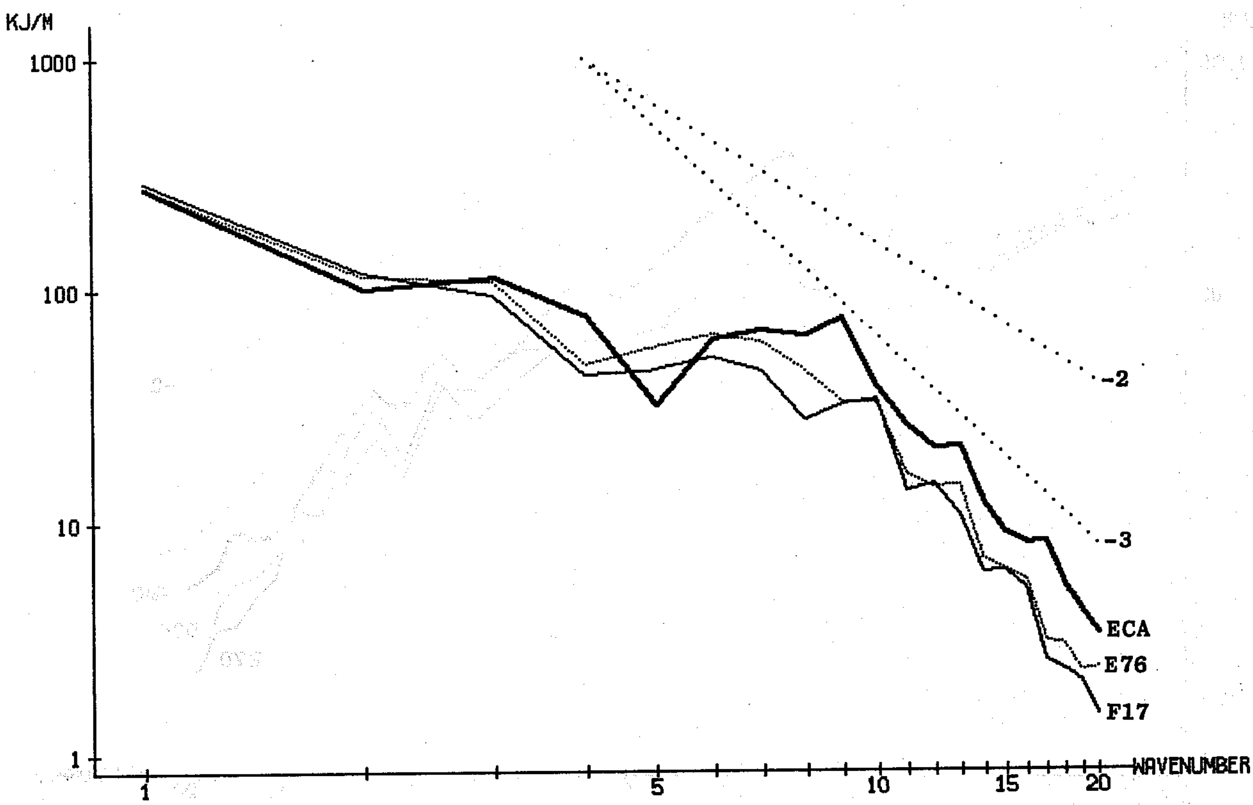

_______ energy conserving .... enstrophy conserving

Fig. 13c As for Fig. 13a but for 22.2.81

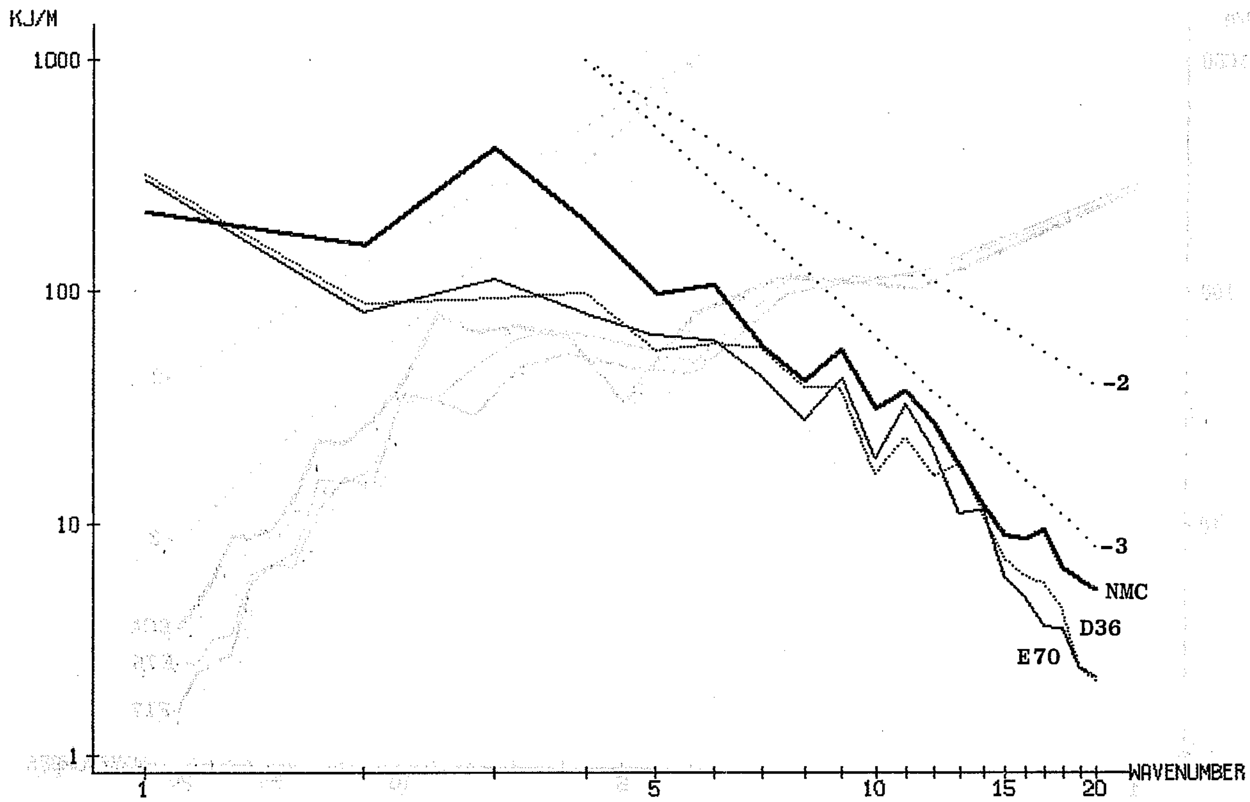

_______ energy conserving .... enstrophy conserving

Fig. 13d As for Fig. 13a but for 1.1.77.

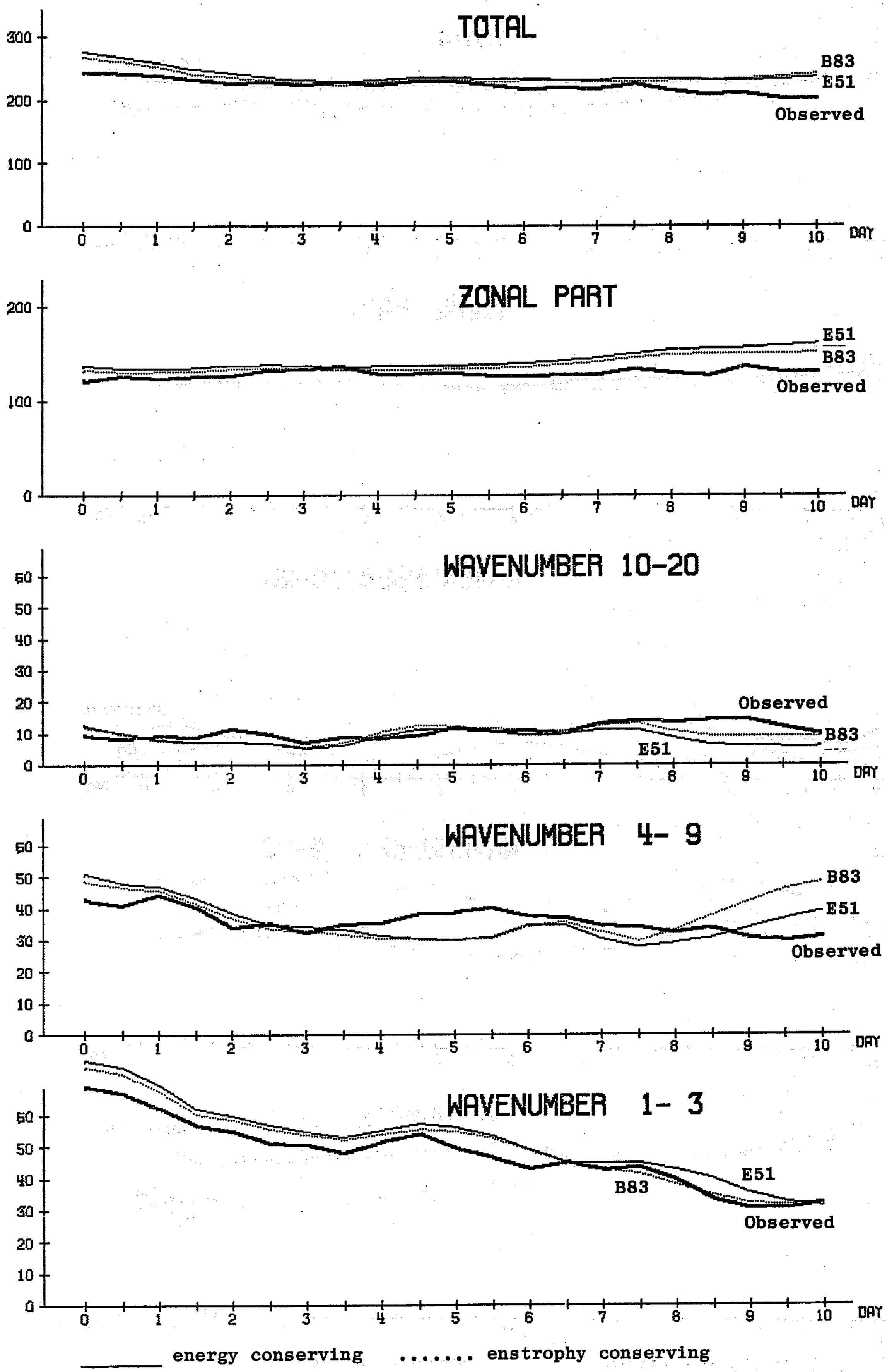

Fig. 14a Time evolution of the kinetic energy for the 16.1.79. Mean between 20 and 82.5°N and over 1000 to 200 mb.

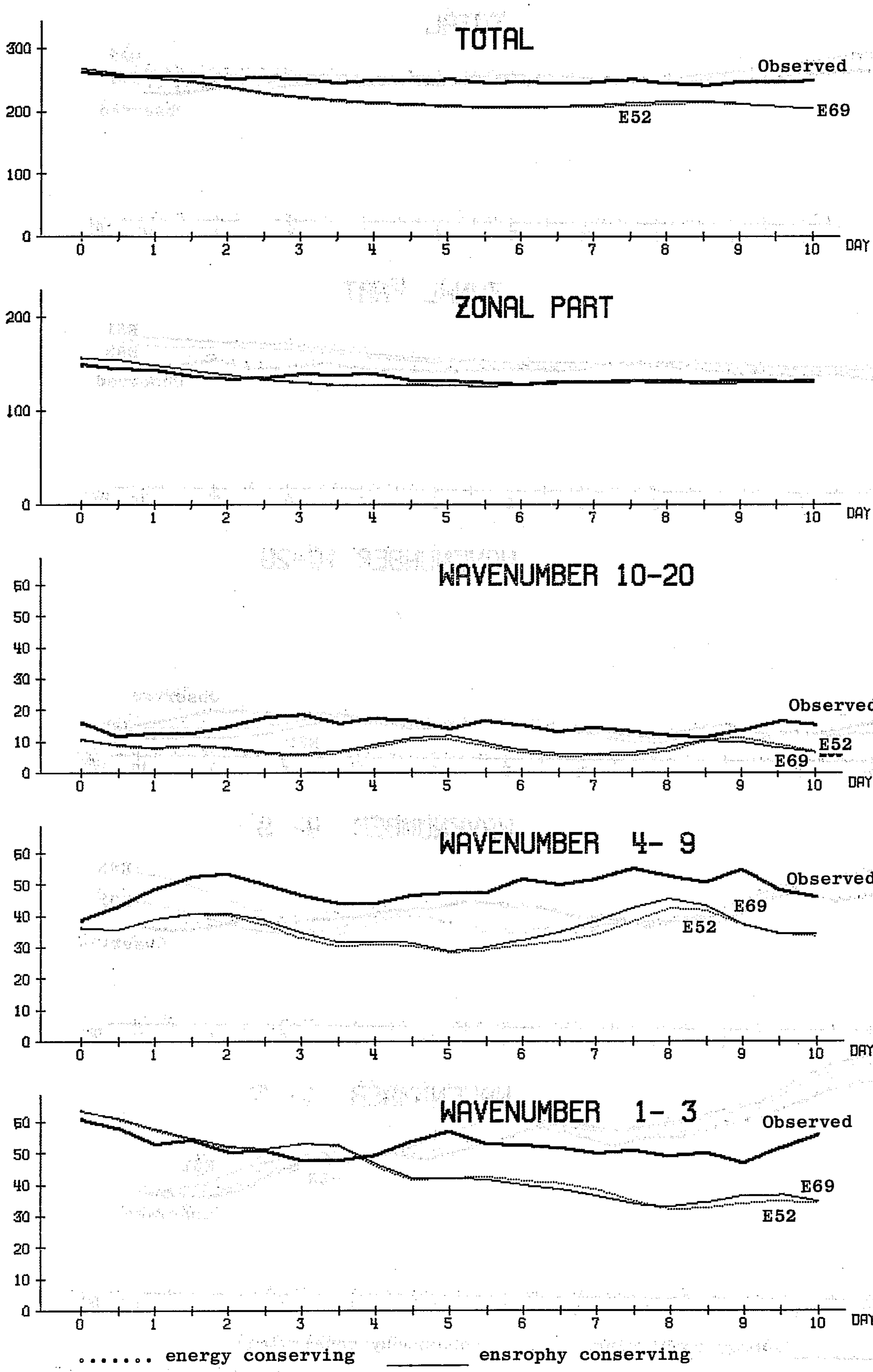

Fig. 14b As for Fig. 14a but for 1.3.65.

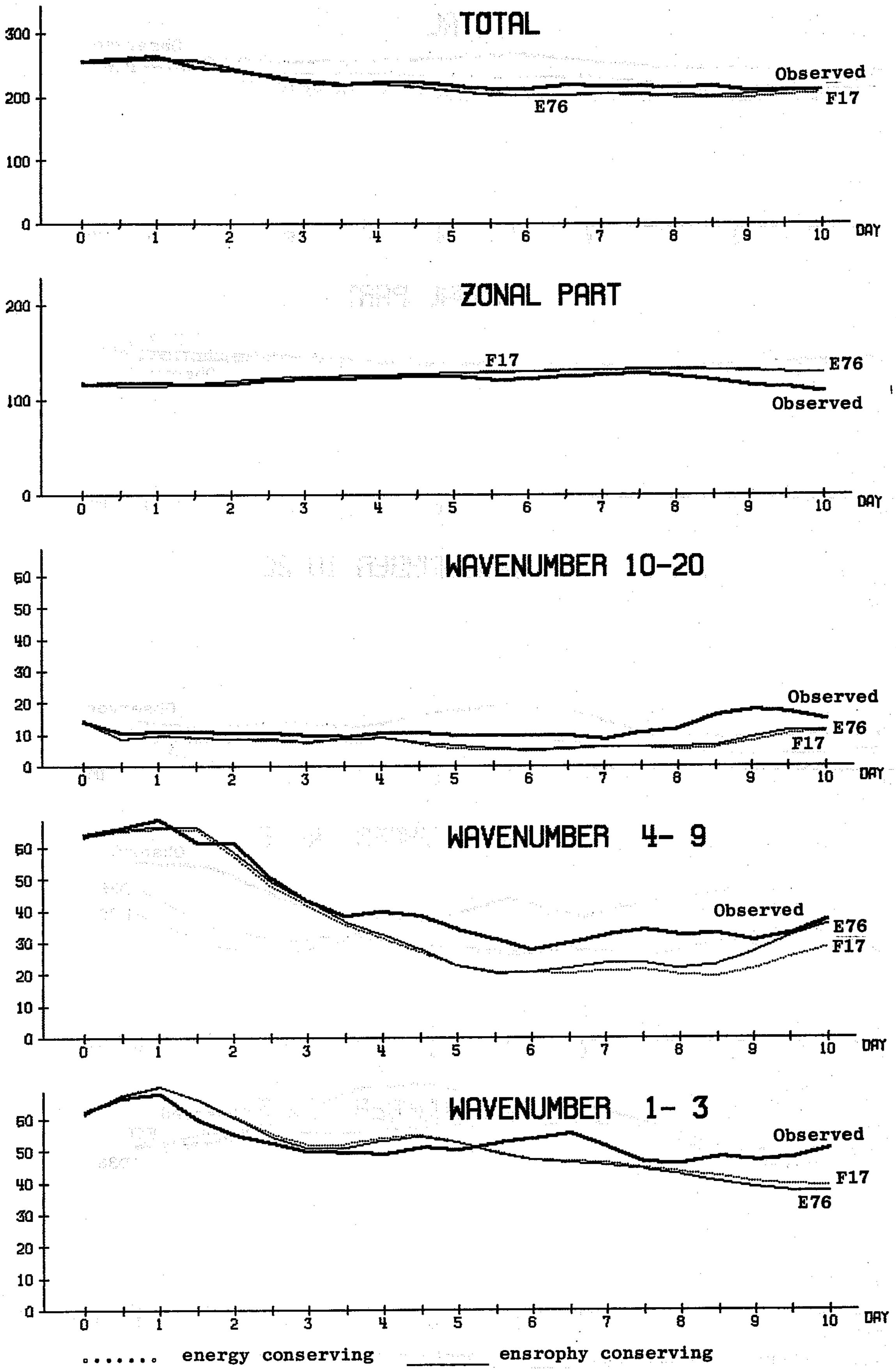

Fig. 14c As for Fig. 14a but for 22.2.81

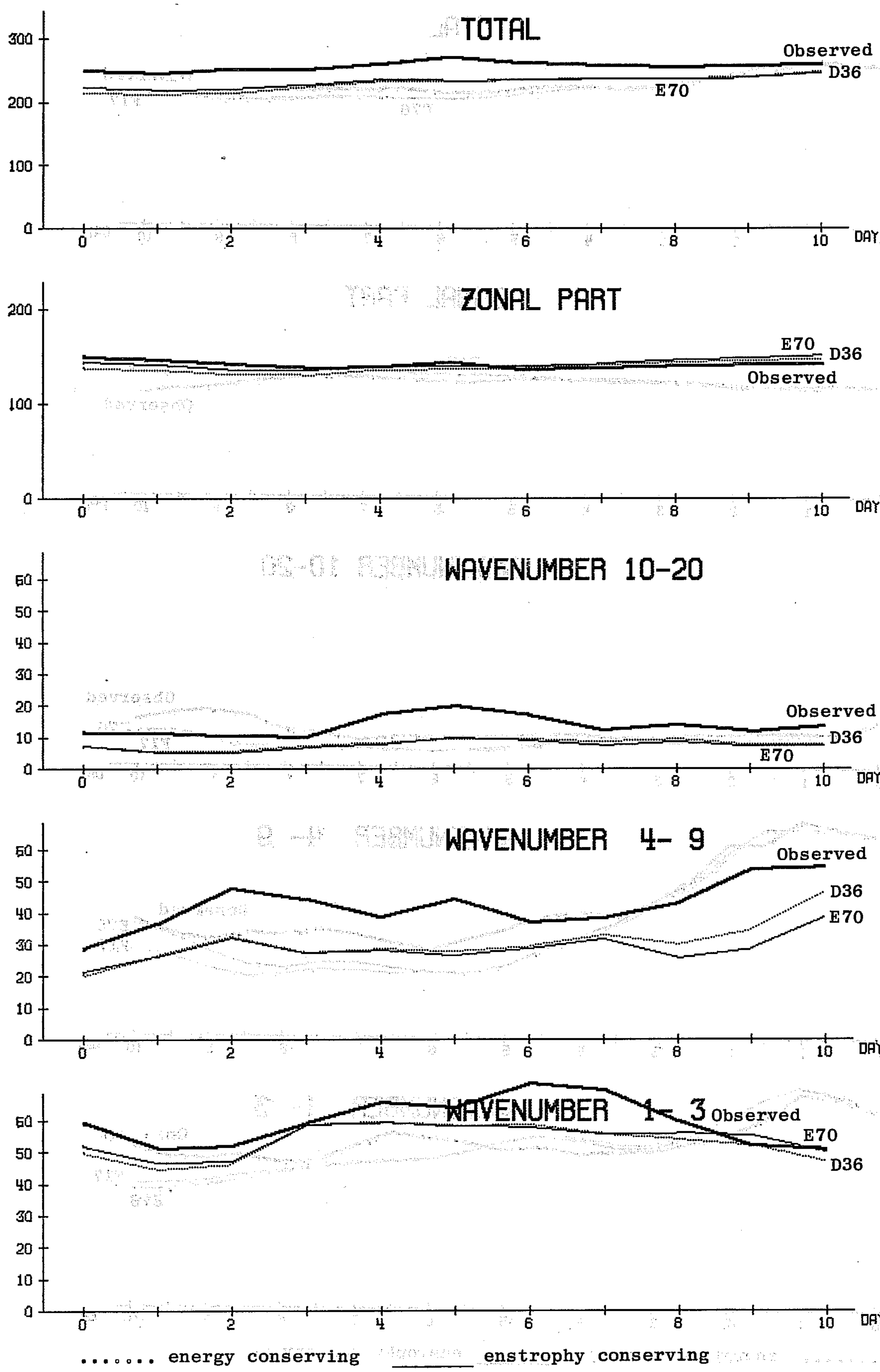

Fig. 14d As for Fig. 14a but for 1.1.77.

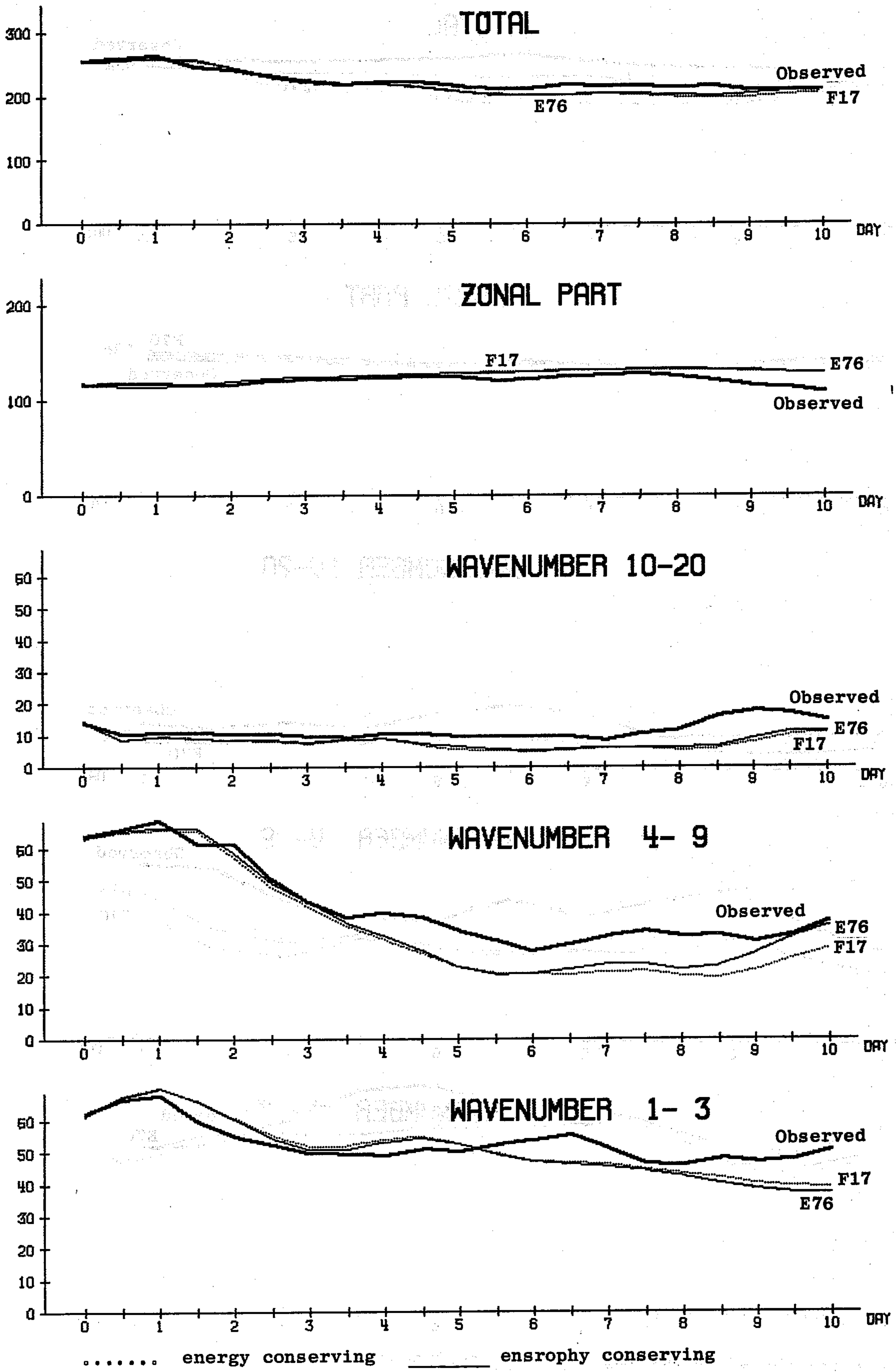

Fig. 14c As for Fig. 14a but for 22.2.81

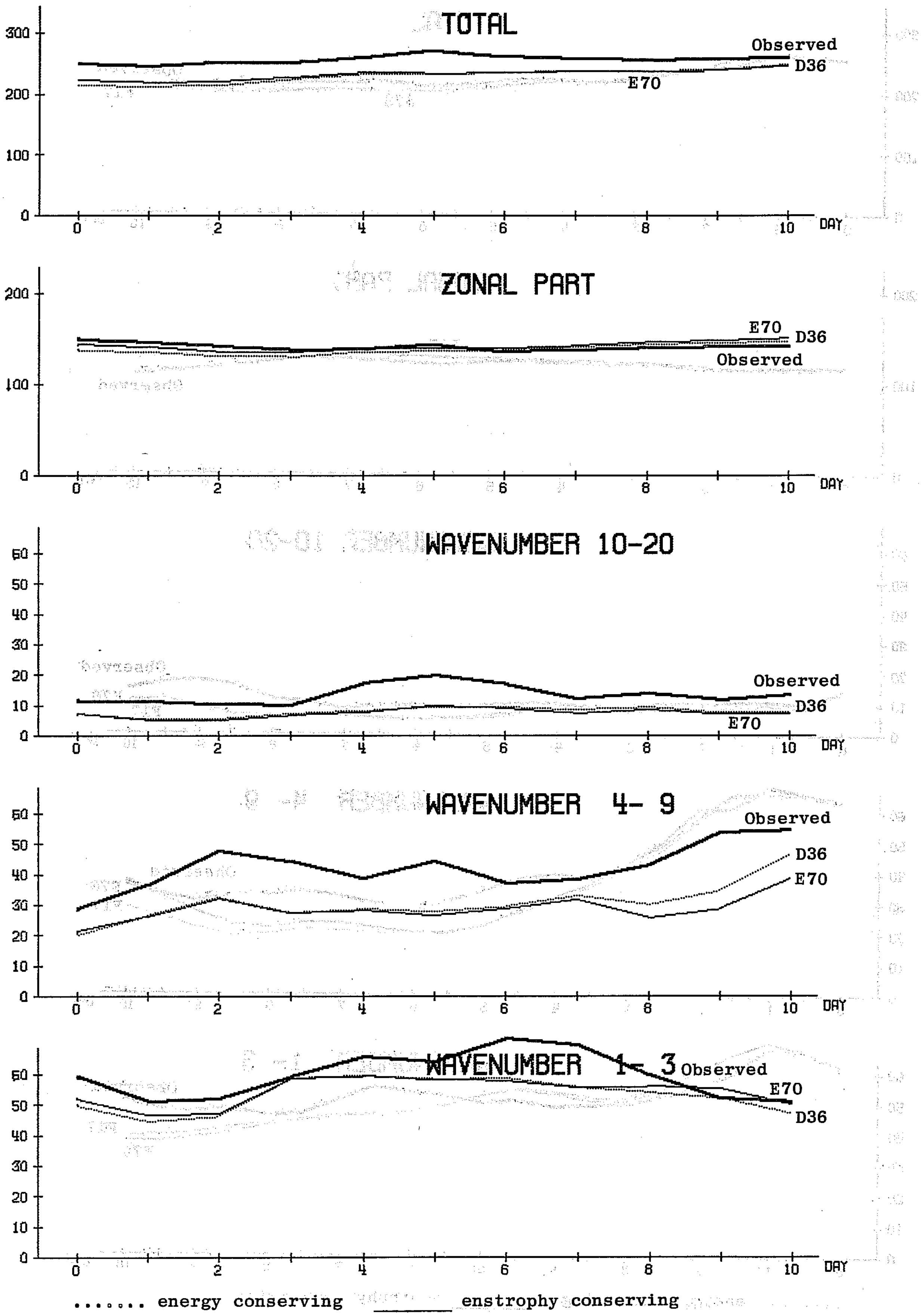

Fig. 14d As for Fig. 14a but for 1.1.77.

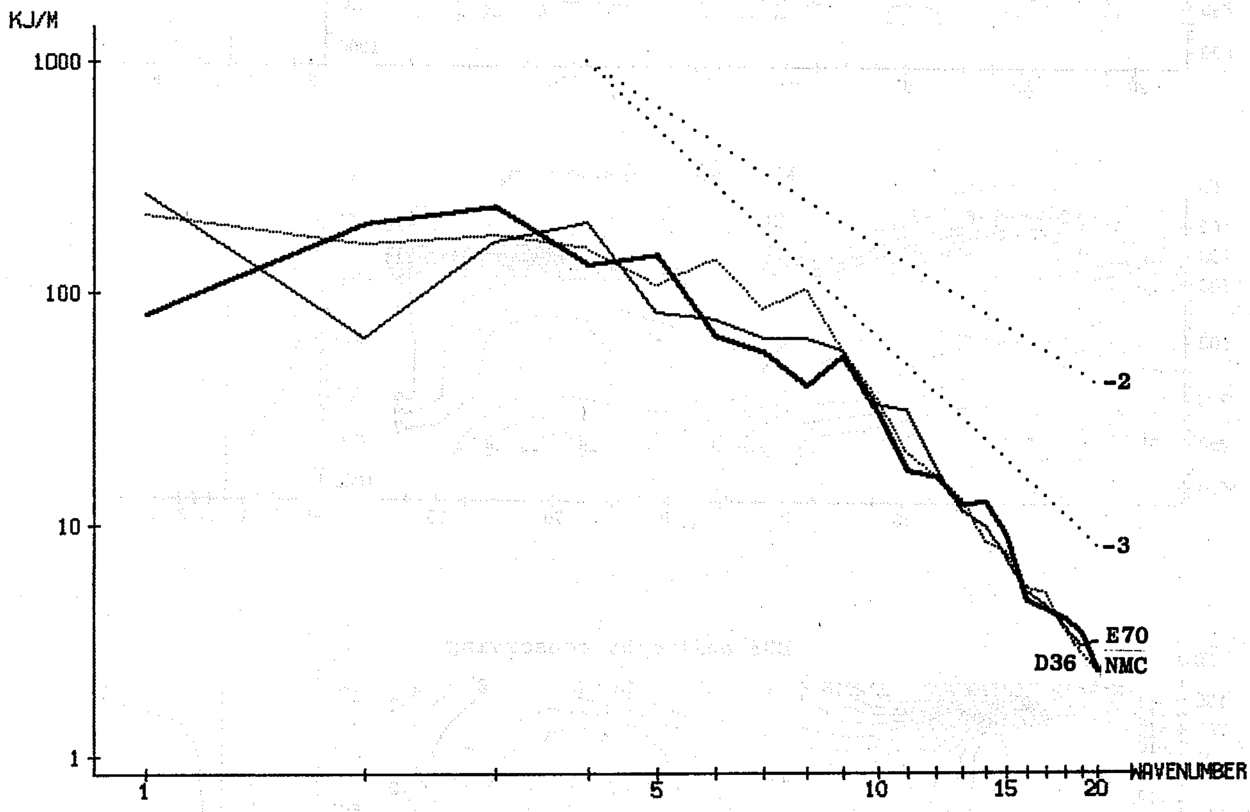

________ energy conserving .... enstrophy conserving

Fig. 15 Spectra of kinetic energy for the 1.1.77 for the second half of the 30 day forecasts of the 1.1.77. Mean between 40 and 60°N and over 1000 to 200 mb.

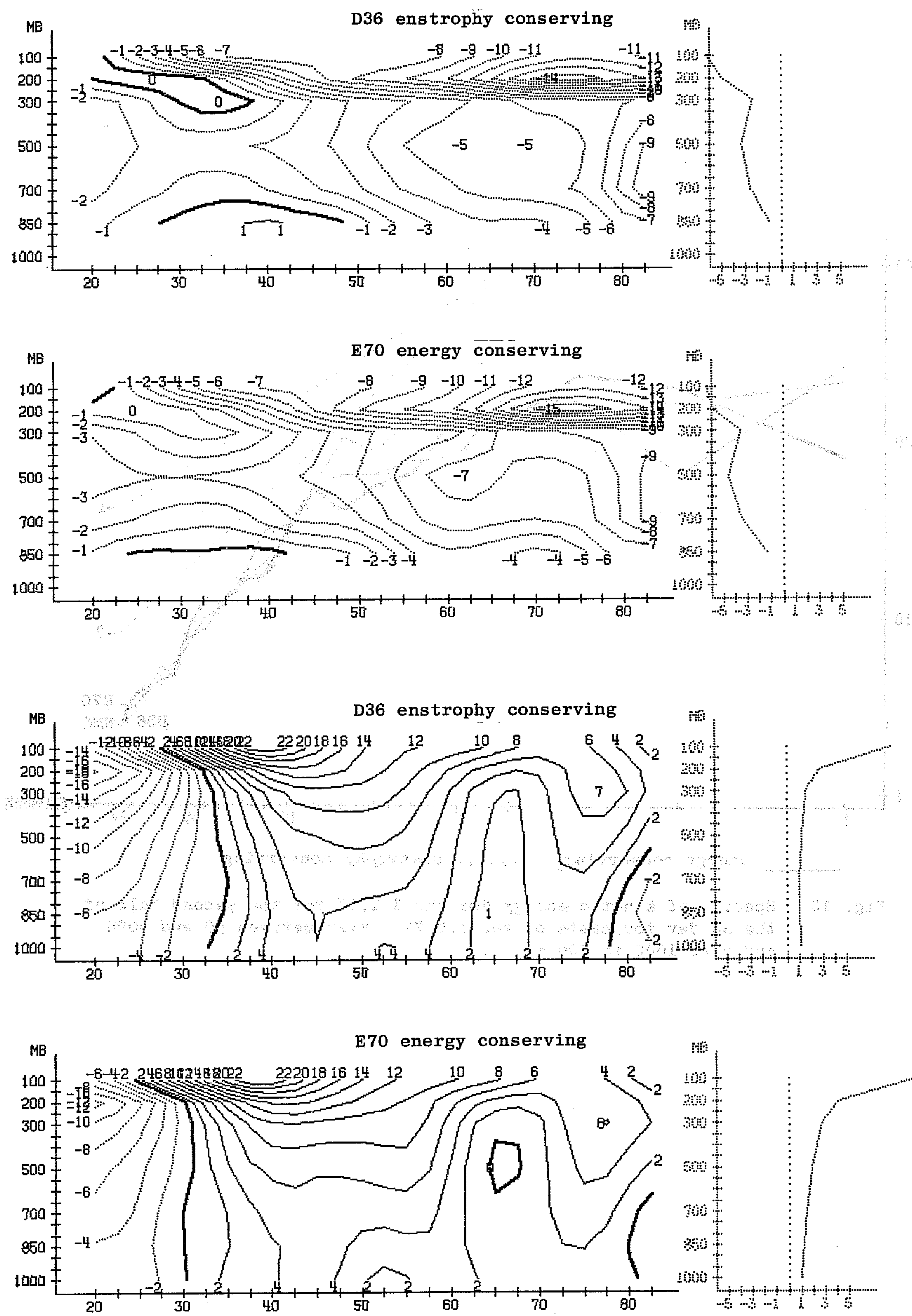

Fig. 16 Latitude height distribution of zonal means of temperature (top) and zonal wind (bottom) deviations from observations for the second half of the 30 day forecasts of the 1.1.77. The small panels to the right show the vertical profile of the area weighted meridional integral of the quantity in the main panel.

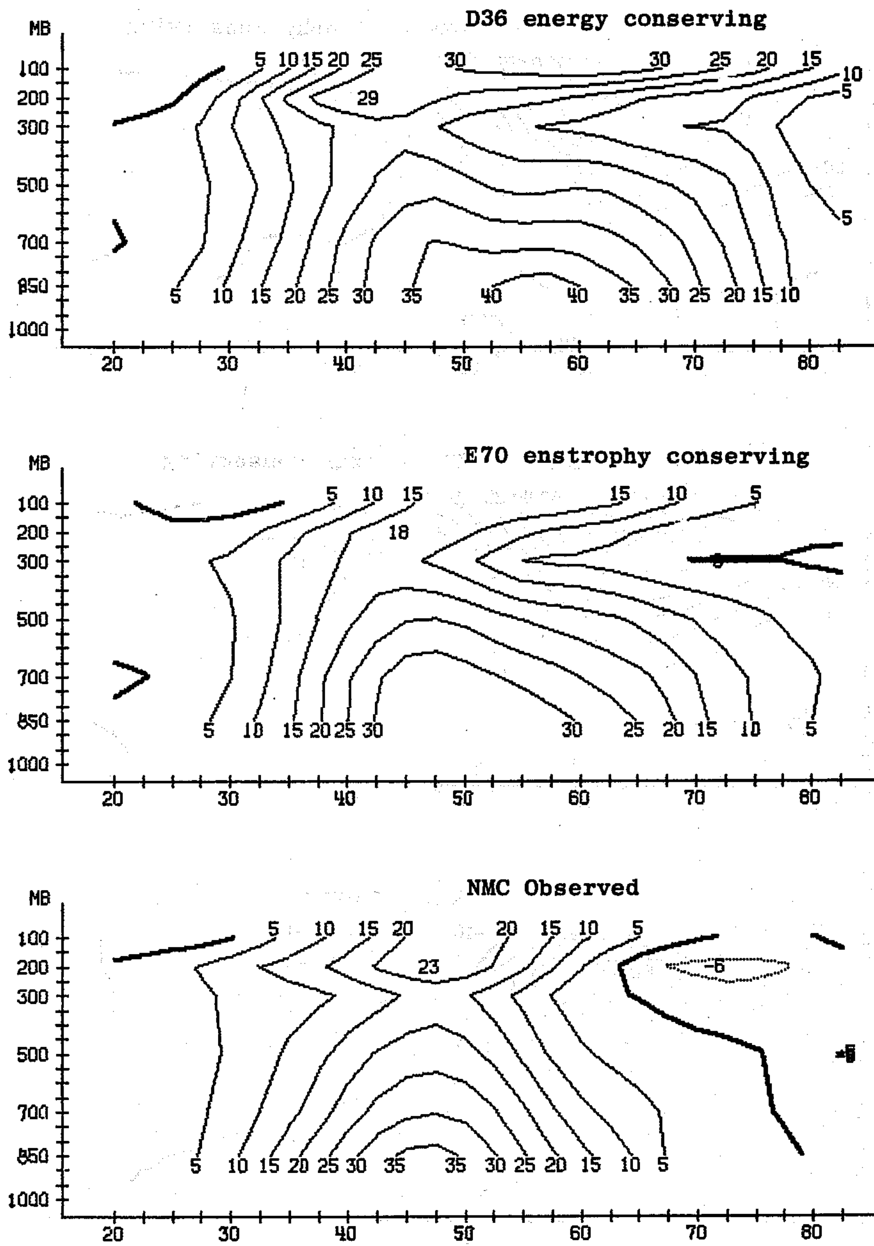

Fig. 17 Latitude height distribution of zonal means of sensible heat flux $\overline{T'V'}$ for the second half of the enstrophy (top), energy conserving 30 day forecast (centre) of the 1.1.77 and the verifying analysis (bottom).

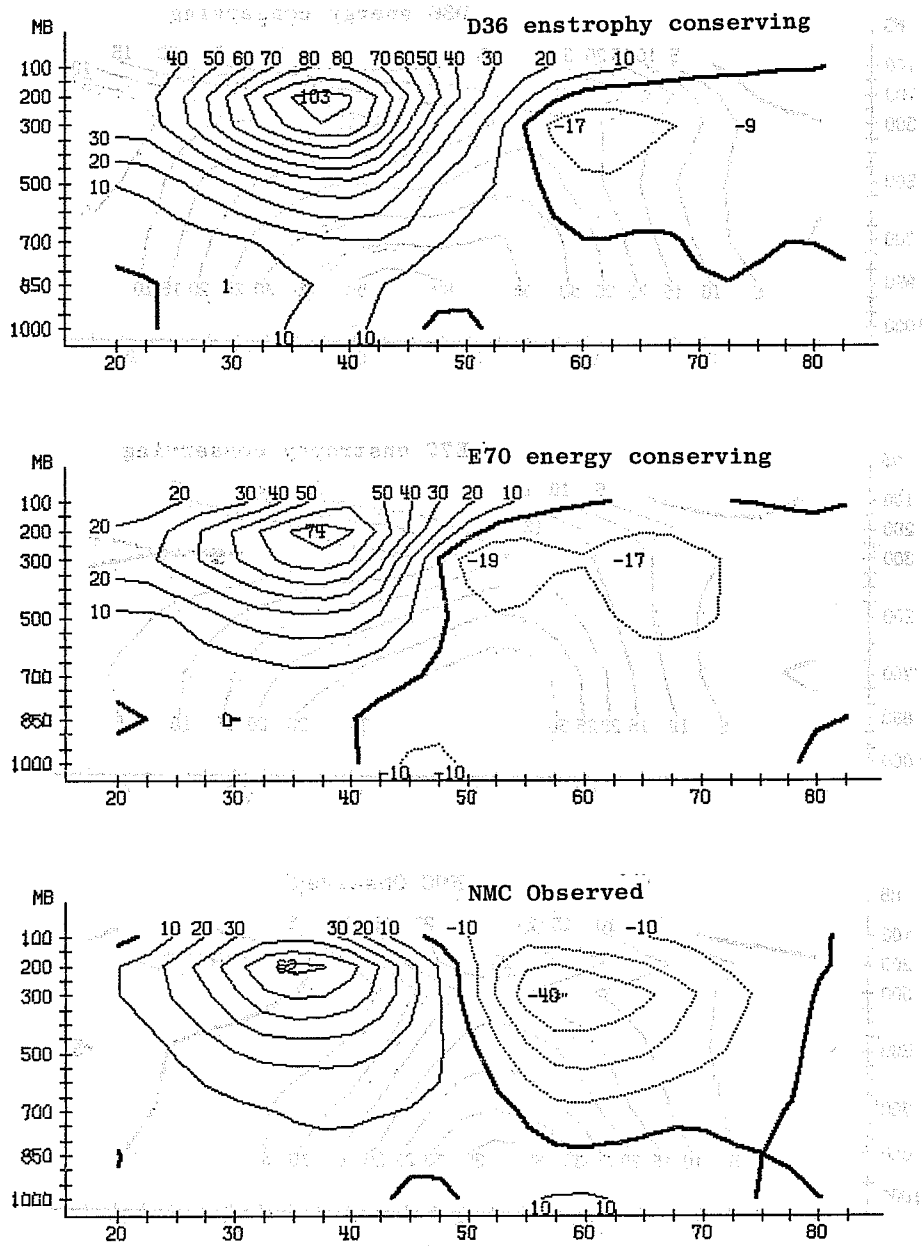

Fig. 18 As Fig. 17, but for momentum flux $\overline{U'V'}$.